

21. PHYSICAL PROPERTIES OF DEEP-SEA SEDIMENTS FROM THE PHILIPPINE SEA AND SEA OF JAPAN

Arnold H. Bouma, Department of Oceanography, Texas A&M University, College Station, Texas
and

J. Casey Moore, Earth Sciences, University of California, Santa Cruz, California

INTRODUCTION

Physical property data were routinely collected on cores recovered during DSDP Leg 31 in the Philippine Sea and Sea of Japan. This paper synthesizes the density, porosity, water content, and vane shear collected in this region. These data are not only of geotechnical significance, but also provide sensitive indicators of physical and chemical diagenesis. It behooves geologists to pay attention to physical properties as they provide quantitative support for many macroscopic to ultra microscopic observations on the sediment-rock transformation.

Wet-bulk density was routinely determined during Leg 31 on at least two sections per core by the Gamma Ray Attenuation Porosity Evaluation (GRAPE). On-board an analog record was produced from which calculations were made for the shipboard reports. The data were also stored on magnetic tape which was processed later via the DSDP facilities. Occasionally a cylinder sample was collected for grain density analyses on shore. Those data were then utilized to correct the assumed grain densities used for the GRAPE. In addition, 1-cc syringe collected samples were taken onboard for direct laboratory analyses of water content, density, and porosity.

Discussions on these measurements are given and/or evaluations have been previously presented (Gealy, 1971; Bennett and Keller, 1973; Boyce, 1973c; Manheim et al., 1974). In addition, a number of memoranda and instructions to the shipboard scientists written by Boyce (1972a, b, c; 1973a, b, d, e; 1974 a, b) present the techniques and the derivation of formulas.

The wide variety of lithologies recovered during Leg 31 provided an opportunity to study the variation of shear strength with sediment type over depths of several hundred meters. These data are compiled by site, and comparisons are made by sediment type.

METHODS, DEFINITIONS, AND EQUATIONS

In the following section some brief notes are given on the methods and evaluations of techniques used, on the definitions of the parameters, and on the equations utilized. Three groups of analyses can be distinguished: (1) water content, density, and porosity via the gravimetric methods; (2) density and porosity via the GRAPE method; and (3) vane-shear measurements.

Gravimetric Methods

No salt corrections are applied in all these techniques. The samples are either collected with a 1-cc syringe for

analyses onboard ship, with a cylinder to provide data for the GRAPE computer program, via a chunk of material if the sediment is too stiff for the syringe method, or in small bottles for home base analyses.

Water Content

Two types of water content data are distinguished: the wet-water content (used throughout this paper) and the dry-water content. These parameters are defined as follows:

$$\begin{aligned} \text{Wet-water content (\%)} &= \\ & \frac{(\text{weight wet sediment}) - (\text{weight dry sediments} + \text{salts})}{(\text{weight wet sediment})} \times 100 \\ &= \frac{(\text{weight of evaporated water})}{(\text{weight of wet sediment})} \times 100 \end{aligned}$$

$$\text{Dry-water content (\%)} = \frac{(\text{weight of evaporated water})}{(\text{weight of dry sediment} + \text{salts})} \times 100$$

If salt corrections (35 ppt @ 21°C) are desired, a factor of 1.0363 may be used with the wet-water content, for example: wet-water content with salt correction = 1.0363 × water content without salt correction (Boyce, 1973a, b; 1974a).

The water content of a 1-cc syringe collected sample was obtained onboard ship. According to Boyce (1974a) the absolute error is about ±2%. This technique can only be applied when dealing with soft sediments which enable the investigator to fill the syringe properly. When this is not successful, a chunk of sample is collected. Not having a known volume is not important when measuring water content.

Occasionally a cylinder sample, about 2½ cm in diameter and 2½ cm high, was collected by the marine technician on watch. This sample is analyzed on shore, and the results are used for the computer program of the magnetic tape GRAPE data. The senior author collected a number of larger samples (about 40-50 cc) in glass bottles for home base analyses. By using large samples and a stable balance, a high accuracy can be obtained.

Wet-Bulk Density

Bulk density or wet unit weight is defined as the ratio of the total weight of the sediment mass to the total volume of the sediment mass irrespective of the degree of saturation (Cernock, 1970). If all voids are filled with

water, the bulk density in g/cc can be calculated according to the equation:

$$\text{Wet-bulk density in g/cc} = \frac{\text{weight of wet sediment}}{\text{volume of wet sediment}}$$

Salt corrections are not required according to Boyce (1973b, 1974b). For these analyses it is vital that the syringe is properly filled and that the volume removed for weighing is cut off very accurately. The volume of 1 cc actually is too small to obtain the accuracies required (Bennett and Keller, 1973). The bottle samples, mentioned under water content, provide much more accurate data.

Porosity

This parameter is defined as the ratio in % of the volume of voids to the total volume of the sediment mass (Cernock, 1970) and it can be calculated from the water content if grain density is known (or can be estimated, and assuming 100% saturation). The porosity can also be obtained from the syringe technique data as follows (no salt correction):

$$\text{Porosity in \%} = \frac{100}{1.00 \text{ g/cc}} \times \frac{\text{weight of evaporated water}}{\text{volume of wet sediment}}$$

Grain Density

The definition of grain density in g/cc is the weight of the mineral grains divided by their volume. This parameter should be calculated from data obtained by the pycnometer method (Boyce, 1973b). Grain density can be calculated as an approximation from the wet-bulk density and the porosity. This is not precise, and it results in a large scatter of data, especially when high porosities are involved. The grain density, including slats, is obtained as follows:

$$\text{Grain density in g/cc} = \frac{(\text{weight of dry sediment} + \text{salts})}{(\text{volume of evaporated water}) (100/\text{porosity}) - (\text{volume of evaporated water})}$$

GRAPE Methods

The GRAPE analog data in the form of magnetic digital tape, was computer processed according to Boyce 1973c (note typographical error in step 2 of Whitmarsh, program on p. 1118 where ρ_{wt} should be ρ_{wt} . Boyce, personal communication).

Sample data, however, were calculated differently than the GRAPE analog data, as follows: gamma rays of a specific energy level are absorbed or scattered when they travel through a core, and the attenuation is related to the density of the sample (Evans, 1965; Harms and Choquette, 1965; Boyce, 1973c). The amount of intensity that is registered can be calculated as follows:

$$I = I_0 e^{-\mu d \rho \beta} \text{ thus } \rho \beta = \frac{1}{\mu d} \ln \left(\frac{I_0}{I} \right)$$

where

I is the intensity of the gamma ray beam penetrating the sample with no loss of energy.

I_0 is the source intensity.

μ is the mass attenuation coefficient in g/cc. Unless the attenuation coefficient of the material is known, the mass attenuation coefficient is 0.100 g/cc.

d is the thickness or diameter of the sample in cm.

$\rho \beta$ is the bulk density in g/cc.

When dealing with porous materials, the above equation becomes (Evans, 1965; Harms and Choquette, 1965; Schlumberger, 1966):

$$\rho \beta = \rho_g (1 - \phi) + \rho_f (\phi)$$

where

ρ_g is the matrix or grain density. Normally the value 2.65 g/cc, the density of quartz, is used. Feldspar and clay densities range from 2.56 to 2.72, calcite 2.71, and dolomite averages 2.85 g/cc. Due to the mixed mineralogy the calculations were based on 2.65 g/cc.

ϕ is the porosity or volume/liquid content when the material is completely liquid saturated.

ρ_f is the density of the fluid filling the pores. The GRAPE value 1.125 g/cc was used. However, the $\rho \beta$ will be in error because the interstitia water attenuation coefficient is greater than that of quartz. Therefore, the analog GRAPE data were processed through the Whitmarsh Iteration for proper adjustment which is equivalent to the following for the sample data:

Assign ρ_f = true density seawater = 1.025 g/cc

Therefore, true wet-bulk density = $\rho_{\beta t}$:

$$\rho_{\beta t} = \rho_g (1 - \phi) + \rho_f (\phi)$$

When combining both bulk-density equations, an equation for porosity is obtained. Using the above-mentioned values, the following simple equation can be derived:

$$\phi = (\rho_g - \frac{1}{\mu d} \ln \frac{I_0}{I}) / (\rho_g - \rho_f)$$

$$\phi = (\rho_g - \frac{1}{\mu d} \ln \frac{I_0}{I}) / (\rho_g - \rho_f)$$

$$\phi = (\rho_g - \rho_{\beta}) / (\rho_g - \rho_f) = \frac{2.65 - \rho_{\beta}}{1.525}$$

VANE SHEAR

Shear strength was determined manually with a "Torvane shear device." The vane shear was rotated at a rate of 10°-20°/sec. All measurements were made by the authors. Repeated determinations by the same or different operators varied by less than 15%. Measurements were made in the least-disturbed portions of the cores, usually near their base and normally on vertical surfaces. All plotted data are from sediment in the clayey silt, silty clay, or clay grain size.

Vane-shear test values provide a measure of sediment cohesion and approximate shear strength determined from unconfined (or confined undrained) triaxial tests.

In this paper only raw values are presented. Lee (1973) has made corrections on vane-shear measurements from North Pacific deep-sea sediments in order to approximate in situ conditions. He finds that the estimated in situ strengths are higher by a factor of 2 or 3 than the laboratory measurements. The uncorrected vane-shear data presented in this paper are referred to simply as shear strength.

**GRAPE COUNT VARIATIONS,
DRIFT CHARACTERISTICS,
AND COMPARISON WITH ANALOG RECORDS**

Two slices of rock from Core 8 (Hole 290) were measured on the GRAPE unit for 2 min according to the count method. The results are presented in Table 1, which not only reveals the variation within one core section of this polymict debris flow deposit (Pluenncke and Bouma, this volume), but also the drift of the equipment.

Two sets of counts were made at slightly different spots on a plan-parallel slice from Piece #1 which is the top piece of Section 1. Eight measurements were carried out at randomly selected spots on a slice from Piece #2 of Section 5. In addition, four repetitive counts were conducted on the same location in this latter slice to find drift characteristics of the unit when measuring inhomogeneous natural material.

Table 1 shows that the drift in the GRAPE system, when the sample is not moving, varies between 6464 and 6651 counts/sec. This is a variation of 187 counts/sec or 2.85% of the average. The drift is 1.50% in the direction of the highest count and 1.39% to the lowest value. Applying these percentage variations to the average number of counts/sec of Piece #2 of Section 5, only 4 counts are higher and 2 counts lower than the range

covered by the variation. This means that 50% of the counts fall within that variation and 50% can be real since the sediment is polymict in nature. The variation is too large to allow conclusions to be drawn about the variations when calculating the resulting densities and porosities.

When comparing these data with the count values obtained from complete core segments, it can be seen that both result in comparable density values. Section 2 has a coarse sandy texture and visually and radiographically is more homogeneous than the much coarser Section 5. This may account for the difference in variation and the difference in counts/sec for both samples.

Instead of using a polymict sediment to study drift characteristics of the GRAPE, the present authors made measurements on a standard aluminum bar with four different thicknesses (1, 1.5, 2, and 2.625 in.) (Table 2). This bar is assumed to be homogeneous, and variations should refer to drift within the unit. The first four measurements in Table 2 were done without moving the bar. The following groups of counts were made while the bar was moving slowly in a horizontal direction. Theoretically, each set of counts covers the same part of the aluminum bar. Table 2 also shows the total variation obtained per groups of counts.

The drift measured when the bar is not moving is much larger than any variation obtained on one thickness from a moving bar. The percentage of variation is higher than the similar one given in Table 1. No comparison can be made between data from the moving and the nonmoving bar. It seems that the variation in number of counts/sec decreases with increasing diameter of the aluminum bar. This may indicate that the accuracy of the measurements increases with a decrease in the length of the air path the gamma rays

TABLE 1
GRAPE Count Measurement on Two Sediment Slices From Core 8,
Hole 290. Based on 2 Minute Counting

Section-Piece	Thickness (cm)	Counts per Sec	Average Counts per Sec	Bulk Density (g/cc)	Porosity (%)	Remarks
1-1	1.6256	6911	6892	2.10	36	D
	1.6256	6872		2.14	33	D
5-2	1.7018	6649	6477	2.23	27.5	D
	1.7018	6610		2.27	25	D
	1.7018	6647		2.24	26.8	D
	1.7018	6236		2.61	2.6	D
	1.7018	6394		2.46	12	D
	1.7018	6437		2.42	15	D
	1.7018	6366		2.49	10	D
	1.7018	6478		2.39	17	D
	1.7018	6464		2.40	16	S
	1.7018	6651		6553	2.38 ^a	17.7 ^a
1.7018	6548	S				
1.7018	6548	S				
	1.7018		6486 ^a			

Note: D indicates that counts were done at different spot from previous one;
S indicates that counts were done at same spot as previous one.

^aTotal average of Piece 2 from Section 5.

TABLE 2
GRAPE Counts on Standard Aluminum Bar With Four Different
Diameters as Used for Calibration Purposes

Thickness (cm)	Counts per 2 sec	Average counts per 2 sec	Average Density (g/cc)	Total Variation (counts per 2 sec) (as % of the average)		Remarks
2.54	4786					Bar not moving
2.54	4686					
2.54	4633	4686	2.874	153	3.27	
2.54	4638					
2.54	4798					Bar moving
2.54	4767	4776	2.799	36	0.75	
2.54	4762					
3.81	3365					Bar moving
3.81	3359	3359	2.790	12	0.36	
3.81	3353					
5.08	2380					Bar moving
5.08	2386	2383	2.768	6	0.25	
5.08	2382					
6.6675	1556					Bar moving
6.6675	1563	1560	2.747	7	0.49	
6.6675	1560					

Note: Mean bulk density for the aluminum bar from these figures is 2.796 g/cc.
Density given by Boyce (1973c, 1973e) is 2.71 g/cc.

have to travel. The distance between the gamma ray source and the scintillation detector is fixed. Accuracy could be improved if the distance of travel through air was fixed, that is, if the cores were of uniform diameter. The analog densities are practically always lower than those obtained from count data.

TEST RESULTS

For geographical as well as lithological purposes, the 12 sites from Leg 31 have been placed into two groups: the Philippine Sea (Sites 290-298) and the Sea of Japan (Sites 299-302). Bulk density, porosity, and water content have been determined by GRAPE and syringe methods on most sites, while vane shear has only been measured at Sites 293, 294, 295, 296, 297, 298, 299, and 302.

Site 290

This site was placed at the distal edge of a sedimentary apron. A significant portion of the sedimentary column was deposited below the carbonate compensation depth and preceded by volcanic debris that have undergone postdepositional alteration.

The upper 90 meters consist predominantly of brown silt-bearing clays, locally becoming silt/zeolite-rich or containing zeolite-rich volcanic ash beds. From 90 to 139 meters the sediments are yellow to medium brown nannofossil oozes, increasing in volcanic ash downward. Locally some radiolarian-bearing/clay-rich zones were observed. From 139 to 225 meters the sediments are mainly zeolite-bearing/ash-rich nannofossil oozes. The bottom part, cored to a depth of 255 meters, consists of volcanic conglomerate containing subangular to sub-rounded clasts of diabase, volcanic alteration products, and glass in a micrite matrix.

The physical properties vary considerably due to the nature of the material as well as to the degree of coring

disturbance. Core 1 was too watery to allow any measurements. Cores 2-6 were dry and core cutting resulted in microfractures which affected the syringe sampling accuracy. Cores 7 and 8 were well indurated.

The data are given in Table 3 and Figure 1. Scattering is large and increase/decrease of bulk density/porosity is small from Cores 1 to 7. A rapid change can be noted in Core 8. The computer plot from the GRAPE data shows little due to a compressed horizontal scale. In Figure 1 the same symbol is used for count method results on pieces from Core 8 as for the syringe method data for the upper seven cores.

Site 291

Two holes, 291 and 291A, were drilled at this site. Five lithologies were distinguished starting with a silt-rich zeolite clay in the upper 69 meters. From 69 to 80 meters a nannofossil ooze was encountered, followed by a clayey radiolarian ooze of late Eocene age to a depth of about 99 meters. This was underlain by a nannofossil-radiolarian-bearing clay changing to a ferruginous, zeolite-rich clay. From 118 to 126.5 meters a fine-grained basalt was drilled.

Few measurements on physical properties were obtained. In most cases the analog record could easily be averaged (Table 4, Figure 2), however, when consistent offsets were recognized, smaller intervals were averaged. The bulk densities thus obtained for Core 5 (Hole 291) were very unreliable due to fragmentation of the material. Therefore, a number of pieces were subjected to the count method. A difference of 0.1-0.2 g/cc was obtained between analog record averaging and count computation, which is within the order of magnitude for technical errors.

A minor, but rather consistent increase in bulk density from 1.28 to 1.42 g/cc was observed in the upper four cores of Hole 291. The basaltic material from Core 5

TABLE 3
Bulk Density, Porosity, and Water Content as Determined by the GRAPE and Syringe Methods, Site 290

Core	Section	Diameter (in.)	Interval (cm)		Lithology	GRAPE		Syringe		Remarks ^b	
			GRAPE ^a	Syringe		Bulk Density (g/cc)	Porosity (%)	Water Content (%)	Bulk Density (g/cc)		Porosity (%)
1	1	2.6	A	66	Silty clay	1.38	83.6	61.29	1.35	82.66	
2	2	2.6	A		Clayey	1.39	82.9				
	3			0-6	Clayey			69.18	1.26	87.03	
				0-6	Clayey			68.81	1.28	87.93	
	4	2.6	A	77	Clayey with volc. ash	1.39	82.9	61.78	1.36	84.20	
	5	2.6	A		Clayey with volc. ash	1.41	80.9				
3	2	2.6	A	74	Nanno and rad ooze	1.42	80.9	59.12	1.32	78.17	
	3	2.6	A	0-6	Nanno ooze	1.41	80.9	52.94	1.40	74.10	
4	2	2.6	A	85	Nanno ooze	1.46	78.3	54.70	1.32	72.20	
5	1			83	Nanno ooze with clay			55.28			Chunk method
				144-150	Nanno ooze with clay			55.46	1.38	76.41	Experimental
	2	2.3	A	143-150	Nanno ooze with clay	1.43	80.3	52.29			Experimental
	3	2.3	0-75		Nanno ooze with clay	1.47	77.6				
		2.3	75-150		Nanno ooze with clay	1.67	64.5				
6	2	2.3	A		Clay-ash-nanno ooze	1.50	75.7				
	3	2.3	A		Nanno volc. ash	1.50	75.7				
7	1			138-150	Nanno volc. ash			44.44	1.25	55.70	Experimental
				138-150	Nanno volc. ash			48.81	1.46	68.46	Experimental
				138-150	Nanno volc. ash			43.97	1.37	60.43	Experimental
	2	2.3	0-75		Nanno volc. ash	1.51	75.0				
		2.3	75-150		Nanno-rich volc. ash	1.58	70.4				
	3	2.3	A		Nanno-rich volc. ash	1.56	71.7				
	4	2.3	A		Nanno volc. ash	1.56	71.7				
			Piece no.					GRAPE count method			
8	1	2.33	2		Volc. conglomerate	2.09	36.8		2.13	34	
		2.32	3		Volc. conglomerate	2.09	36.8		2.08	37	
		2.32	4		Volc. conglomerate	2.07	38.2		2.15	32.7	
		2.32	5		Volc. conglomerate	2.14	33.6		2.17	31	
	2	2.32	1		Volc. conglomerate	2.06	38.8		2.07	38	
		2.32	14		Volc. conglomerate	2.10	36.2		2.24	26.8	
		2.33	16		Volc. conglomerate	2.12	34.9		2.17	31	
		2.30	19		Volc. conglomerate	2.17	31.6		2.24	26.8	
	3	2.32	4		Volc. conglomerate	2.23	27.6		2.34	20	
		2.33	9		Volc. conglomerate	2.23	27.6		2.27	25	
		2.32	11		Volc. conglomerate	2.04	40.1		2.12	34.7	
		2.32	12		Volc. conglomerate	2.06	38.8		2.12	34.7	
		2.32	14		Volc. conglomerate	2.18	30.9		2.27	25	
		2.32	15		Volc. conglomerate	2.20	29.6		2.27	25	
		2.32	17		Volc. conglomerate	2.16	32.2		2.23	27.5	
	4	2.30	4		Volc. conglomerate	2.11	35.5		2.19	20	
		2.32	6		Volc. conglomerate	2.31	22.4		2.39	17	
		2.32	17		Volc. conglomerate	2.31	22.4		2.39	17	
		2.30	18		Volc. conglomerate	2.56	5.9		2.66	-	
	5	2.30	1		Volc. conglomerate	2.39	23.0		2.49	10	
		2.34	6		Volc. conglomerate	2.41	15.8		2.47	11	
		2.335	15		Volc. conglomerate	2.53	7.9		2.60	3	

^aA = average reading from the GRAPE analog record.

^bExperimental = all weighings made on triple beam balance. Volume was determined by subtracting the weight in water from the wet weight.

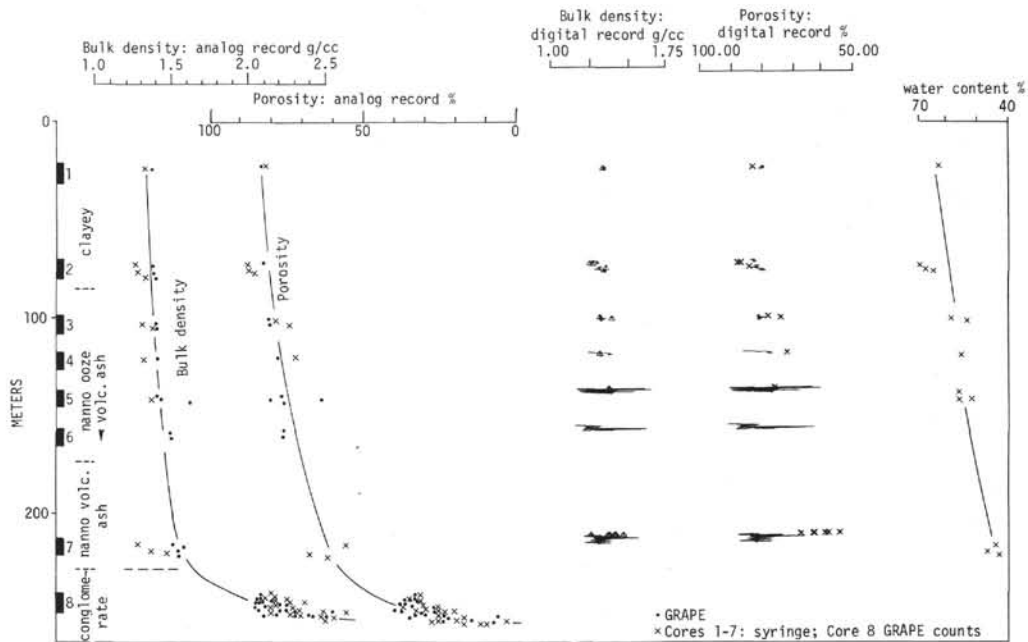


Figure 1. Plot of physical properties for Site 290. GRAPE analog record readings as well as computer plot are presented in addition to laboratory analyses (syringe and chunk methods). On the left the cores are given as black rectangles and the general lithology.

TABLE 4
Bulk Density, Porosity, and Water Content as Determined by the GRAPE and Syringe Methods, Site 291

Core	Section	Diameter (in.)	Interval (cm)		Lithology	GRAPE		Syringe		Remarks	
			GRAPE ^a	Syringe		Bulk Density (g/cc)	Porosity (%)	Water Content (%)	Bulk Density (g/cc)		Porosity (%)
1	1			140	Silty zeolite clay			56.92	1.38	78.5	
2	1			144-150	Silty zeolite clay			56.52	1.41	79.8	
	2	2.6	A		Nanno ooze	1.28	89.8				
3	1			136	Clayey rad ooze			76.02	1.19	90.2	
4	2	2.6	A		Clay	1.28	89.8				
	3	2.6	0-70		Zeolite-rich clay	1.33	86.6				
		2.6	90-125		Rad zeolite clay	1.37	83.9				
		2.6	130-150		Rad zeolite clay	1.42	80.7				
	4	2.6	A	0-6	Cherty clay	1.37	83.9	46.28	1.49	68.8	
				0-6	Cherty clay			56.64	1.31	74.2	
				88	Zeolite clay			62.10	1.31	81.4	
5	2	2.34	Piece no.		Basalt	2.96					Count method
		0.27	4		Basalt	3.04					Count method
		2.35	7A-1		Basalt	2.87					
		2.35	7B		Basalt	2.87					
		2.35	12		Basalt	2.82					
		2.35	16		Basalt	2.82					
		2.35	16		Basalt	3.01					Count method

^aA = average reading from the GRAPE analog record.

reveals a much higher density (2.82-2.87 g/cc on the analog record and 2.96-3.04 g/cc via the count method).

The water content values vary between 46% and 76% in the upper four cores with no apparent pattern. The value seems out of proportion in Core 3, presumably due to the sloppy consistency as a result of drilling distortion.

The porosities and water content show a reversal in a downward direction. With increase in radiolarian content an increase in porosity and water content can be observed. If this is real or artificial cannot be determined here.

Site 292

Site 292 was drilled to a depth of 443.5 meters through 367.5 meters of nannofossil ooze and chalk. The upper 154 meters consist of ooze, from 154-225 meters the sediment consists of nannofossil ooze with interbedded nannofossil chalk, while the bottom 142.5 meters were made up of nannofossil chalk with minor interbeddings of nannofossil ooze and cherty concretions. Below this, starting with Core 40 a sequence of exceptionally uniform intersertal to subophitic tholeiitic basalts were drilled.

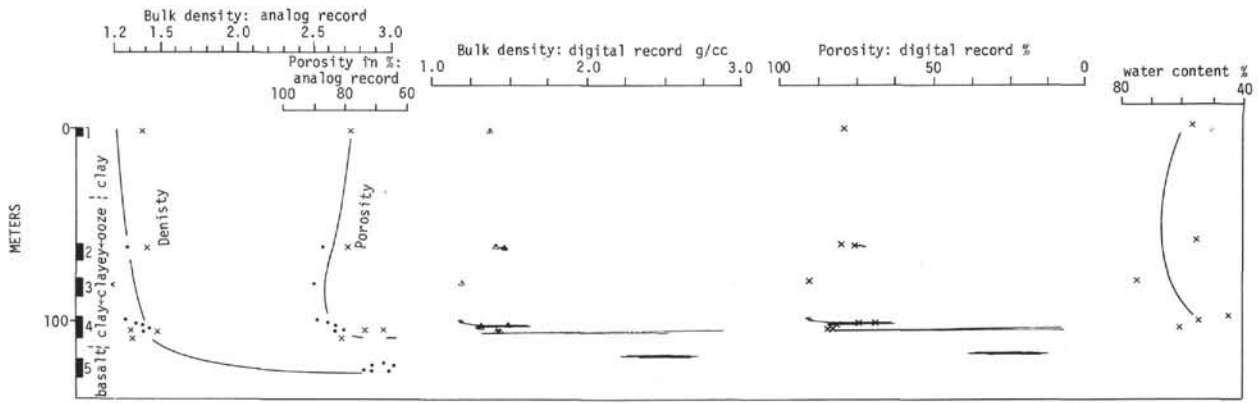


Figure 2. Plot of physical properties for Site 291. GRAPE analog record readings as well as computer plot are presented in addition to laboratory analyses (syringe and chunk methods). On the left the cores are given as black rectangles and the general lithology.

Most of the core sections were homogeneous enough to allow averaging of the GRAPE analog curve. Except for a few points, the scattering of data (Table 5, Figure 3) is small in the upper 160 meters. With increase in induration, an increase of irregularities can be observed (Table 5) and a larger scattering (Figure 3). Variations in the amount of foraminifera, radiolarians, clay, and volcanic ash primarily account for the variations in bulk density and porosity. It is also in this sediment packet, between 275 and 265 meters, that the increase of the mean bulk density is not associated with a decrease in water content.

With a few minor exceptions the laboratory-derived bulk density values are always lower than the GRAPE analog readings. Part can be due to drift in the GRAPE, but most differences must be a result of the syringe/chunk method which collects too small a sample to be completely representative of the larger part of the core or section. In addition, it is difficult to collect a good syringe sample from the easily ruptured ooze and chalk.

Figure 3 shows a steady, but small, increase/decrease of the bulk density/porosity with depth.

Site 293

Drilling and interval coring were carried out at Site 293 to a depth of 563.5 meters. Eighteen cores were recovered from the sediment column overlying basalt. No sediment was recovered from Core 1.

The sediment column consists of clay with sand, sandy silt, sandy clay, silty clay, and clayey silt intercalations as is common for a turbidite type series. With depth in the hole there is a decrease of the coarser components. The basaltic breccia is overlain by red deep-sea clay which in turn is covered by a grayish clay.

The physical properties are listed in Table 6 and the plots are presented in Figure 4. The scattering of the GRAPE plots is minor in spite of the lithological variations. An overall increase/decrease of bulk density/porosity occurs in the sediment column with depth. A sudden jump can be observed between the densities of the lower muds and the underlying basalts. Figure 4 also

presents slightly lower/higher values for the density/porosity between the gray clayey muds of Cores 15 and 16 and the red deep-sea clays of Core 17.

The data obtained from the syringe method reveal a broader scatter than similar data determined by the GRAPE. This is to be expected when dealing with non-homogeneous sediments in which the GRAPE data present averaged values per core section, while the syringe values represent point data.

Vane Shear

Only six vane-shear measurements were made on the cores from this site. In general the shear strength increases in a downward direction (Table 7). The grossly anomalous values are apparently due to inconsistencies in the measuring technique or a weakening of the cores by drilling fluid. Not enough points are present in Figure 5 to draw a realistic enveloping curve. Although a general increase in strength with depth is visible, about 33% of the points fall completely outside an average curve.

Sites 294 and 295

These two sites were drilled in the same general area about 1.8 km apart. Seven cores were recovered from Site 294 from a depth below the sea floor of 0-118 meters. Site 295 was cored between 101 and 158 meters, resulting in 4 cores. The location was in the low-relief undulating topography of the northeastern part of the West Philippine Basin. The entire 100-150 meters of pelagic cover over the acoustic basement consist of brown clay, slightly calcareous near the base, which possibly overlies basalt. The clay is estimated to have an accumulation rate of 2.0-2.5 m/m.y., including a consolidation factor.

In most instances the GRAPE data were sufficiently homogeneous to allow averaging for density and porosity. In general, the clayey sediments of Sites 294/295 are of low density and high porosity, reflecting their poor consolidation (Tables 8 and 9; Figure 6). A minor increase/decrease in density/porosity can be observed downhole. However, these trends are flat or even show a minor reversal in Cores 1-3 at Site 295. This may be a

TABLE 5
Bulk Density, Porosity, and Water Content as Determined by the GRAPE and Syringe Methods, Site 292

Core	Section	Diameter (in.)	Interval (cm)		Lithology	GRAPE		Syringe		Remarks ^b							
			GRAPE ^a	Syringe		Bulk Density (g/cc)	Porosity (%)	Water Content (%)	Bulk Density (g/cc)		Porosity (%)						
1	1	2.6	A	10	Nanno ooze	1.60	68.9	47.12	1.51	71.3	Chunk method						
	3			104	Clayey-glass ooze							46.99	1.53	71.7			
	4			110	Nanno ooze							43.29	1.57	68.1			
2	1	2.6	A	130	Foram-nanno ooze	1.75	59.0	42.85	1.58	67.6							
	2			144-150	Clayey foram-nanno ooze							46.21	1.54	71.0			
3	3	2.6	A	80	Clayey foram-nanno ooze	1.55	72.1	43.36	1.34	58.1							
	2			0-75	Clayey micarb							1.62	67.5				
	2			75-150	Clayey micarb							1.96	45.2				
4	3	2.6	A	70	Volc. ash clayey micarb	1.67	64.3	40.78	1.62	66.2							
	4				A							Clayey ooze	1.69	63.0	41.37	1.60	66.3
	1				A							Nanno ooze	1.66	64.9			
	2				A						Nanno ooze	1.66	64.9				
	3				A						Nanno ooze	1.68	63.6				
5	4	2.6	A	100	Nanno ooze	1.66	64.9	36.69	1.66	61.0							
	5				A						Nanno ooze	1.73	60.3	38.20	1.64	62.8	
	2				0-75						Nanno ooze	1.68	63.6				
6	2	2.6	A	53	Nanno ooze	1.74	59.7	38.20	1.64	62.8							
	5				A						Nanno ooze	1.70	62.3	36.69	1.66	61.0	
	5				A						Nanno ooze	1.70	62.3	38.37	1.65	63.5	
7	6	2.6	A	51	Nanno ooze	1.70	62.3	41.75	1.61	67.0							
	2				0-6						Nanno ooze	1.70	62.3	41.53	1.58	65.6	
	5				A						Nanno ooze	1.70	62.3	36.25	1.69	61.9	
8	5	2.6	A	50	Nanno ooze	1.70	62.3	36.61	1.64	60.2							
	2				0-75						Micarb nanno ooze	1.71	61.6				
	2				75-150						Micarb nanno ooze	1.92	47.9				
9	5	2.6	A	55	Micarb nanno ooze	1.74	59.7	35.55	1.73	61.6							
	2				A						Nanno ooze	1.76	58.4	36.88	1.65	60.9	
	5				A						Nanno ooze	1.79	56.4	33.42	1.73	57.7	
10	2	2.6	A	80	Nanno ooze	1.75	59.0										
11	2	2.6	A	75	Nanno ooze	1.79	56.4	32.47	1.74	56.7							
	5				A						Nanno ooze	1.78	57.0	32.75	1.77	57.9	
12	3	2.6	A	144-150	Foram-nanno ooze	1.79	56.4	32.10	1.73	55.7							
	4				A						Foram-nanno ooze	1.81	55.1				
13	2	2.6	A	78	Foram-nanno ooze	1.76	58.4	31.62	1.63	51.7							
	2				A						Foram-nanno ooze	1.76	58.4	30.06	1.68	50.4	
14	5	2.6	A	90	Foram-nanno ooze	1.80	55.7	30.90	1.77	54.8							
	2				A						Nanno ooze	1.65	65.6				
	5				A						Nanno ooze	1.79	56.4				
15	3	2.6	A	75	Nanno ooze	1.87	51.1	33.08	1.68	55.5							
	4				A						Nanno ooze	1.78	57.0				
16	6	2.6	A	45	Nanno ooze	1.62	67.5	33.07	1.75	58.0							
	4				A						Foram-nanno ooze	1.79	56.4	30.20	1.76	53.2	
	5				A						Foram-nanno ooze	1.79	56.4	30.20	1.76	53.2	
17	6	2.6	A	136	Foram-nanno ooze	1.67	64.3	36.26	1.68	60.9							
	5				A						Foram-nanno ooze	1.67	64.3	36.26	1.68	60.9	
	6	2.6	A	72	Foram-nanno ooze and ash	1.85	52.5	32.67	1.73	56.7							

18	5	2.6	A	68	Nanno ooze, chalky	1.79	56.4	33.77	1.74	58.8	
	6	2.6	0-100	49	Nanno ooze, chalky	1.79	56.4	32.48	1.66	54.0	
		2.6	100-150		Nanno ooze, chalky	1.74	59.7				
19	2	2.6	A	75	Nanno ooze, chalky	1.79	56.4	30.64	1.80	55.1	
	5	2.6	A	49	Nanno ooze, chalky	1.80	55.7	32.52	1.66	54.1	
20	2	2.6	0-75		Nanno ooze, chalky	1.72	61.0				
		2.6	75-100	80	Nanno ooze, chalky	1.80	55.7	30.73	1.76	54.1	
21	4			144-150	Nanno ooze, chalky			33.03	1.99	65.8	
	5	2.6	A	122	Nanno ooze, chalky	1.71	61.6	32.12	1.65	53.2	Chunk method
		2.6	75-80		Nanno ooze, chalky	1.78	57.0				
22	3	2.6	0-50		Ash nanno ooze	1.67	64.3				
		2.6	50-150	106	Ash nanno ooze	1.71	61.6	31.07	1.64	50.9	Chunk method
23	3	2.6	A		Chalky nanno ooze	1.80	55.7				
	4	2.6	A	74	Chalky nanno ooze	1.85	52.5	31.38	1.76	55.2	
24	2	2.6	A		Chalky nanno ooze	1.76	58.4				
	3	2.6	A	78	Chalky nanno ooze	1.80	55.7	31.40	1.69	52.9	Chunk method
25	1			111	Chalky nanno ooze			30.66	1.66	50.9	Chunk method
26	1			144-150	Nanno chalk			28.85	1.77	51.1	Chunk method
	2			107	Nanno chalk			29.28	1.78	52.0	Chunk method
27	1			87	Nanno chalk			27.58	1.76	48.7	Chunk method
29	1			104	Nanno chalk			29.31	1.71	50.2	Chunk method
30	1	2.4	0-50		Nanno chalk	1.84	53.1				
		2.15	50-100		Nanno chalk	2.02	41.3				
		2.2	100-150	102	Nanno chalk	1.97	44.6	29.52	1.69	49.8	Chunk method
31	2	2.33	A	144-150	Nanno chalk	1.86	51.8	28.64	1.80	51.5	Chunk method
32	1	2.42	A		Nanno chalk	1.89	49.8				
33	1			26	Nanno chalk			22.77	1.55	35.4	Chunk method
	2	1.82	A		Nanno chalk	2.13	34.1				
		2.32	A		Nanno chalk	2.19	30.2				
34	1	2.6	A	96	Nanno chalk	1.76	58.4	25.04			Chunk method
35	2	2.38	A	20	Nanno chalk	2.16	32.1	18.67			Chunk method
36	1	2.2	A		Nanno chalk	2.13	34.1				
	3	2.2	A	142-150	Nanno chalk	1.89	49.8	32.48	1.70	55.1	Chunk method
	5	2.3	A		Rad-nanno chalk	2.16	32.1				
37	2			122	Nanno chalk			28.06	1.82	51.0	Chunk method
	3	2.6	A		Ash nanno chalk	1.85	52.5				
38	2	2.6	0-75	54	Nanno micarb chalk	1.75	59.0	27.22	1.82	49.5	Chunk method
		2.6	75-100		Nanno micarb chalk and ash	1.79	56.4				
39	3	2.3	A	50	Foram micarb nanno chalk	2.25	26.2	17.35	1.99	34.5	Chunk method
40	1	2.34	A		Basalt	2.68					
42	3	2.34	75-150		Basalt	2.68					
44	5	2.35	A		Basalt	2.69					
46	2	2.30	A		Basalt	2.76					
47	2	2.35	A		Basalt	2.72					

^aA = average reading from the GRAPE analog record.

^b₁) = end of syringe was not covered properly, end of sample may have lost some water.

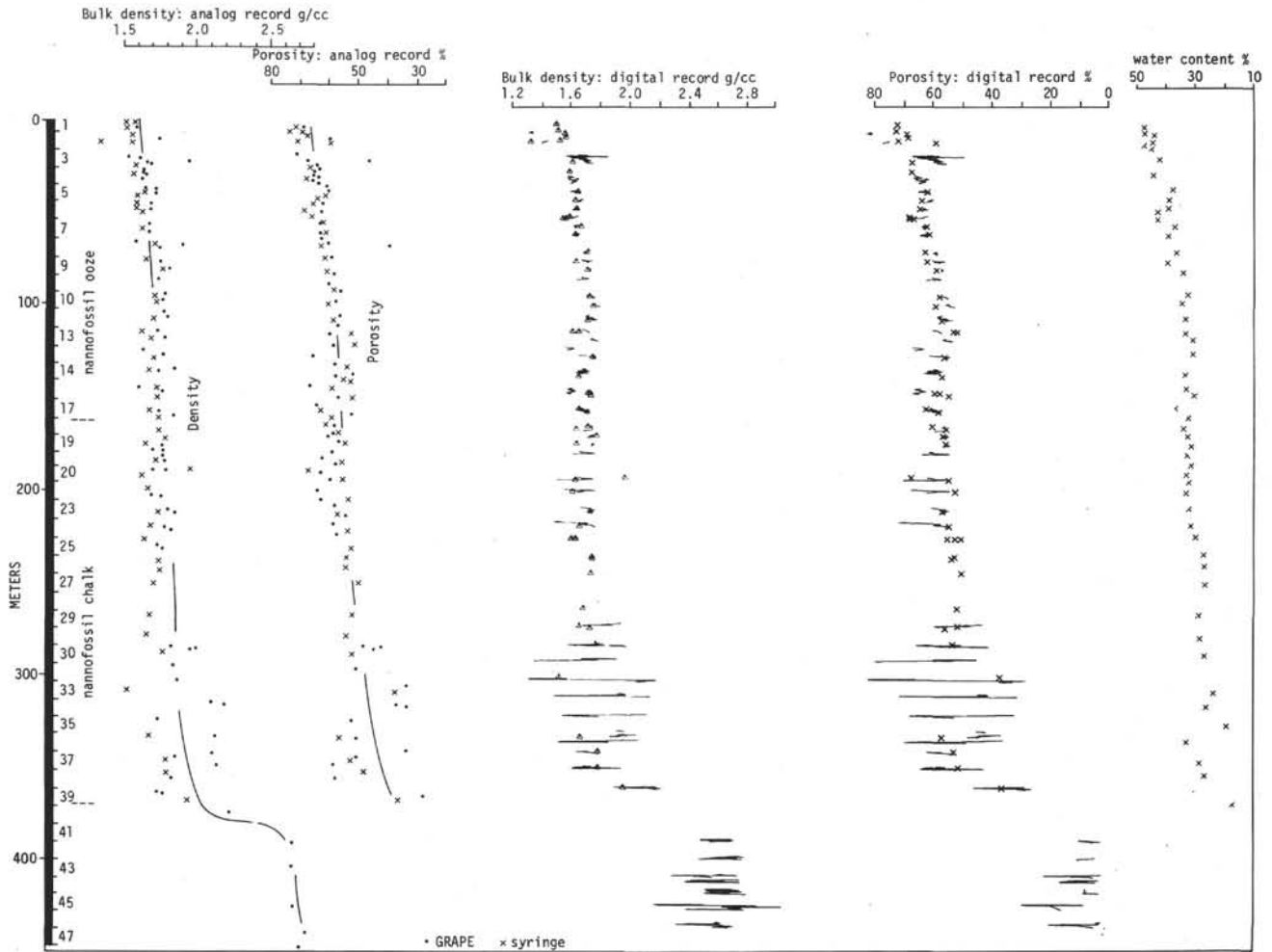


Figure 3. Plot of physical properties for Site 292. GRAPE analog record readings as well as computer plot are presented in addition to laboratory analyses (syringe and chunk methods). On the left the cores are given as black rectangles and the general lithology.

result of the greater drilling disturbances observed in the cores from Site 295 compared to Site 294.

The syringe data for density and porosity correlate closely with the GRAPE analog readings. The water content plot reveals more scattering and a general decrease downhole with a possible exception for the values from Site 295.

Vane Shear

The vane-shear data for Site 294 (Figure 7, Table 10) show the least variation for a given depth of any sequence cored during Leg 31. This result is due in part to the homogeneous lithology as well as minor remolding during coring. The enveloping curve is unusual in that it shows a concave upward shape.

In the same figure the data for Site 295 are presented (see Table 11). The scatter in these data is also thought to be the result of more intense drilling disturbance. As a result the data from Site 294 are considered to be more valuable and more indicative for the shear strength in this brown clay.

Site 296

Site 296 was primarily intended as a biostratigraphic hole. Located at the northern end of the Palau-Kyushu Ridge, the site had to be at a depth substantially shallower than the calcium carbonate compensation depth, far enough north to produce a midlatitude flora and fauna, and beneath sufficiently productive waters.

A total of 65 cores were retrieved over a depth range of 0-1087 meters below the sea floor. The upper 48 cores (depth 0-453 m) consist of Pleistocene to late Oligocene nanofossil oozes and chalks with varieties including clay, forams, radiolarians, or ash-bearing/rich and volcanic ash beds. In general, the volcanic activity decreased from late Oligocene to the Holocene, being replaced by a pelagic nanofossil sedimentation.

Radiolarians are present in the upper portions of the cored interval. They become absent with increasing depth and reappear again in Cores 22-38. Foraminifera are also variable in their content but occur down to Core 56.

TABLE 6
Bulk Density, Porosity, and Water Content as Determined by the GRAPE and Syringe Methods, Site 293

Core	Section	Diameter (in.)	Interval (cm)		Lithology	GRAPE		Syringe		Remarks	
			GRAPE ^a	Syringe		Bulk Density (g/cc)	Porosity (%)	Water Content (%)	Bulk Density (g/cc)		Porosity (%)
2	4			144-150				42.70	1.51	64.4	
	5	2.6	A	144-150				32.31	1.71	55.2	
3	3	2.6	A	75		1.79	56.4	42.60	1.57	66.7	
	5	2.6	A	100		1.50	75.4				
4	1			144-150		1.68	63.6	33.73	1.70	57.3	
	2	2.6	A	45		1.68	63.6	35.31	1.69	59.8	
5	4	2.6	A	60		1.65	65.6	36.59	1.68	61.6	
6	2			102				33.94	1.61	54.6	
7	1	2.6	A			1.65	65.6	36.38	1.65	60.2	
	2			144-150				39.12	1.60	62.7	
8	6	2.6	A			1.65	65.6				
9	1			144-150				30.11	1.74	52.5	
	2	2.6	A	10		1.65	65.6	34.20	1.63	55.9	
	6	2.6	A			1.76	58.4				
10	2			144-150				33.60	1.66	55.9	
	3	2.6	A	144-150				34.32	1.70	58.3	
12	2	2.6	A			1.74	59.7				
	3	2.6	A			1.87	51.1				
13	1			144-150							
	2	2.6	A	144-150				32.04	1.76	56.4	
15	1			130				17.21	2.06	35.4	
	3			144-150		1.75	59.0				
	4	2.6	A	130		1.86	51.8	29.64	1.86	46.8	
16	5	2.6	A	8		1.84	53.1	25.20	1.86	46.8	
17	4			144-150				29.91	1.73	51.7	
	5	2.6	A			1.76	58.4	30.91	1.72	53.2	
18	1	2.6	0-100			1.86		36.42	1.67	60.8	
	2	2.32	100-150			2.62					
20	1	2.2	A			2.58					
			Piece no.								
		2.15	2		Basaltic breccia	2.64					Count method
		2.12	5		Basaltic breccia	2.61					Count method
		2.09	7		Basaltic breccia	2.65					Count method
		2.1	16		Basaltic breccia	2.50					Count method
		2.2	18		Basaltic breccia	2.60					Count method
21	2	2.32	A		Basaltic breccia	2.62					Count method

^aA = average reading from the GRAPE analog record.

From 453-1087 meters a mixture of tuffs, lapilli tuffs, volcanic sandstones, and siltstones and occasional ash-rich/bearing nannofossil chalks were encountered. This lower section especially illustrates a continued building up by accumulation of volcanic debris with accompanying subsidence of the Palau-Kyushu Ridge. Sedimentation breaks occur in the Miocene section (Cores 23-35).

The bulk density, porosity, and water content data, as presented in Table 12 and Figure 8, reveal that the density values obtained by the syringe method are almost always lower than the GRAPE analog readings. Although the position of the syringe is arbitrarily picked, it presents a point data and is too small in volume for accuracy. Figure 8 shows that, with a few exceptions, the scattering is low and that only a minor change with depth occurs. No significant difference can be seen between the nannofossil ooze, nannofossil chalk, and the ash-rich/bearing nannofossil chalk. Water content data reveal the same overall trend.

Vane Shear

The vane-shear measurements (Figure 9, Table 13) increase rapidly along a well-defined trend to 50 meters. At greater depths the data show more scattering and the rate of strengthening decreases. The variation in shear strength from 50 to 155 meters is in part due to drilling deformation, but also may be a function of periodic variation in natural consolidation-lithification factors at depths greater than 100 meters.

Site 297

This site was located on the outer swell of the Nankai Trough with a sediment cover typical of the western Shikoku Basin. In total, 27 cores were collected representing 679.5 meters of sediment. The upper 54 meters are characterized by a diatom/ash-rich clay that changes into a clay-rich nannofossil ooze for the next 36 meters, followed by 240 meters of clayey siltstone. This material becomes a silty claystone with interbedded

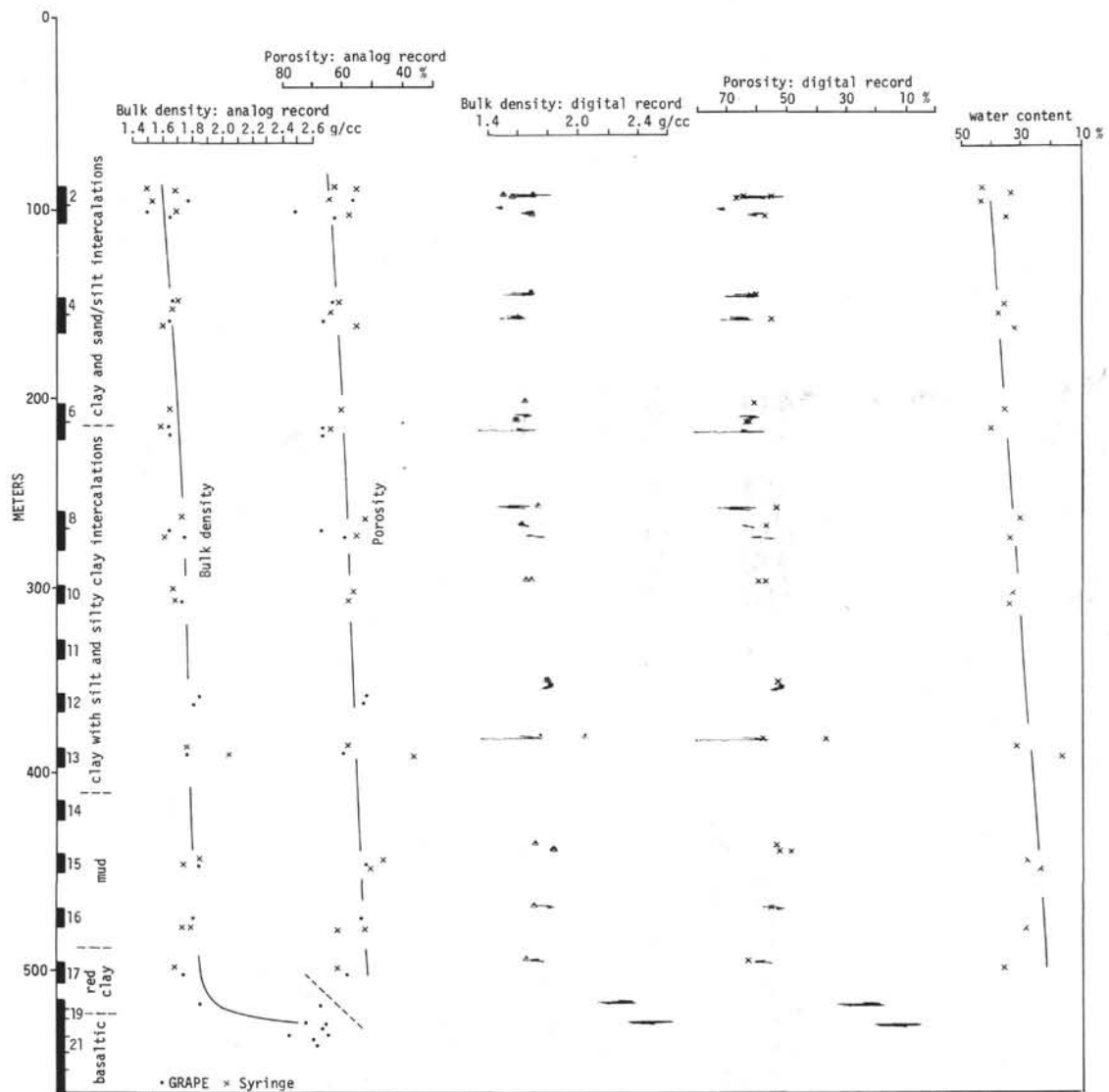


Figure 4. Plot of physical properties for Site 293. GRAPE analog record readings as well as computer plot are presented in addition to laboratory analyses (syringe and chunk methods). On the left the cores are given as black rectangles and the general lithology.

TABLE 7
Vane Shear Data, Site 293

Sample (Interval in cm)	Depth (to nearest half meter)	Plane of Measurement	Shear Strength (mbars)
2-5, 80	96.5	Vertical	195.3
3-5, 100	106.0	Vertical	527.3
4-2, 150	158.0	Horizontal	332.0
5-4, 150	161.5	Horizontal	214.8
6-2, 150	205.5	Horizontal	507.8
12-0, 0	354.5	Vertical	703.1

graded silt and sand in Cores 14-22 representing the 330-570 meter depth. This is underlain by a fine vitric ash and ash-rich claystone.

Most core sections revealed a rather straight analog GRAPE curve, and the average could be used to determine the bulk density. Some sections gave very irregular curves making it difficult to select the most representative value. The laboratory analyses may not have been as accurate as on previous sites due to rougher seas. This induced rolling and additional vibration may account for the anomalously high laboratory density measurements relative to the GRAPE values.

The results are given in tabulated form in Table 14 and graphically in Figure 10. Although the average gives the normal increase/decrease in density/porosity-water content, a number of zones fall too far outside the mean-

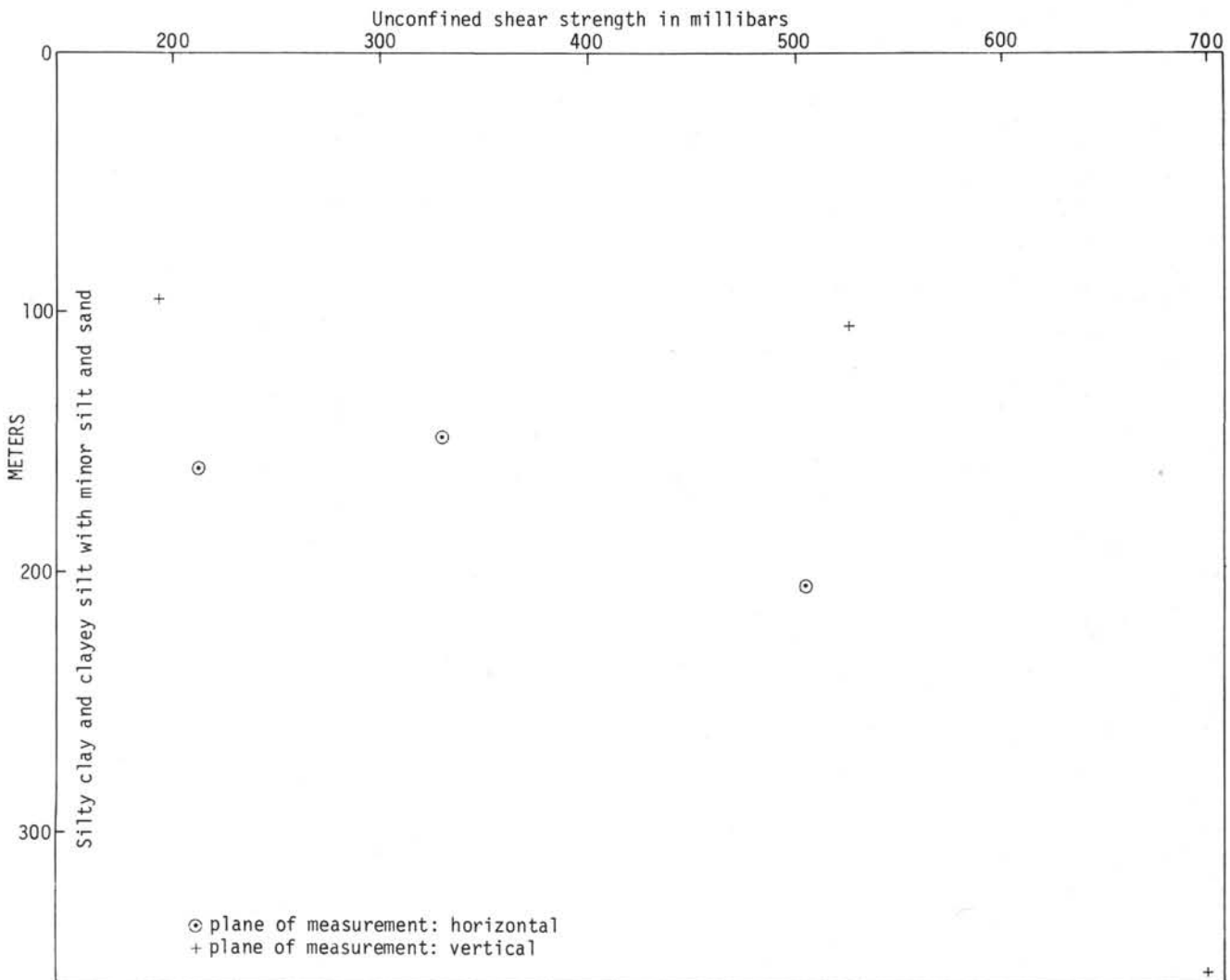


Figure 5. Plot of unconfined shear strength with depth, Site 293.

line to be considered as scattering. Figure 10 shows that all data points fall left of the mean for Cores 9-13, after which a sudden jump to the right occurs. Except for one density analog reading in Core 20, this right-side position continues down to Core 24. A change in lithology from clay to a sandy-silty clay probably accounts for this. Part of the scattering in this lithological unit results from the layering of graded silts and sand in the claystone. This is not visible in the water-content column due to less data points based on samples that were collected in claystone only.

A sudden change is seen when entering the lowest unit. Within this unit a downward increase in clay was observed which influences the values of the physical properties.

Vane Shear

The diatom-ash nannofossil-rich silty clays cored at this site comprise a typical hemipelagic sediment. The shear strength of these deposits (Figure 11, Table 15) increases approximately linearly to 125 meters. At greater

depths the enveloping curve steepens and reflects a concave downward shape.

Site 298

In total, 611 meters were drilled with a recovery of 16 cores. Site 298 was located on the lowermost inner trench wall of the western Nankai Trough. This feature is thought to represent a recently rejuvenated deep-sea trench and a line of subduction. The prime objective at this site was to obtain a representative sample of deformed trench fill.

The upper four cores recovered predominantly a silty clay and clayey silt with varying amounts of sand and minor quantities of calcareous sandstone and limestone. Underneath this lithological unit the influence of the subduction could be observed by the shaly character of the sediment. The lithologies varied between fissile claystone, silty claystone, siltstone, and clayey and silty sands. The overconsolidation of the clay was remarkable (Trabant et al., this volume). In contrast with the fissile claystone and silty claystones, the sand

TABLE 8
Bulk Density, Porosity, and Water Content as Determined by the GRAPE and Syringe Methods, Site 294

Core	Section	Diameter (in.)	Interval (cm)		Lithology	GRAPE		Syringe			Remarks
			GRAPE ^a	Syringe		Bulk Density (g/cc)	Porosity (%)	Water Content (%)	Bulk Density (g/cc)	Porosity (%)	
1	3	2.6	A		Silt-rich clay	1.14	99.0				
	4	2.6	A	75	Silt-rich clay	1.20	95.1	57.22	1.37	78.2	
2	1			144-150	Clay			71.31	1.25	89.1	
				144-150	Clay			72.46	1.20	87.1	
				90	Clay	1.23	93.1	67.36	1.30	87.3	
3	2	2.6	A		Clay	1.27	90.5				
	4	2.6	A	144-150	Clay			62.03	1.33	82.2	
	5	2.6	A	40	Clay	1.26	91.1	40.06	1.57	78.8	
4	3	2.6	A	90	Clay			65.77	1.26	83.1	
		2.6	0-100		Clay	1.33	86.6				Irregular
		2.6	100-150	144-150	Clay	1.57	70.8				
6	1	2.6			Clay	1.40	82.0	50.54	1.56	78.7	
		2.6	0-75		Clay	1.40	82.0				
		2.6	75-150	60	Clay and volc. ash	1.63	66.9	59.94	1.35	80.7	Average of peaks

^aA = average reading from the GRAPE analog record. Irregular = irregular analog record.

TABLE 9
Bulk Density, Porosity, and Water Content as Determined by the GRAPE and Syringe Methods, Site 295

Core	Section	Diameter (in.)	Interval (cm)		Lithology	GRAPE		Syringe			Remarks
			GRAPE ^a	Syringe		Bulk Density (g/cc)	Porosity (%)	Water Content (%)	Bulk Density (g/cc)	Porosity (%)	
1	3	2.6	A	30	Clay and volc. ash	1.44	79.3	53.36	1.42	75.7	
	4	2.6	A	143-150	Clay and volc. ash	1.45	78.7	50.82	1.49	75.6	
2	2	2.6	A	40	Clay and volc. ash	1.35	85.2	55.38	1.40	77.5	
	5			144-150	Clay and volc. ash			59.05	1.36	80.3	
3	6	2.6	A	110	Clay and volc. ash	1.37	83.9	59.17	1.37	81.1	
	2	2.6	A		Clay	1.34	85.9				
	3	2.6	A	40	Clay	1.34	85.9	61.64	1.36	83.6	
4	4	2.6	A	144-150	Clay			59.00	1.37	80.9	
				40	Clay	1.37	83.9	58.11	1.40	81.4	

^aA = average reading from the GRAPE analog record.

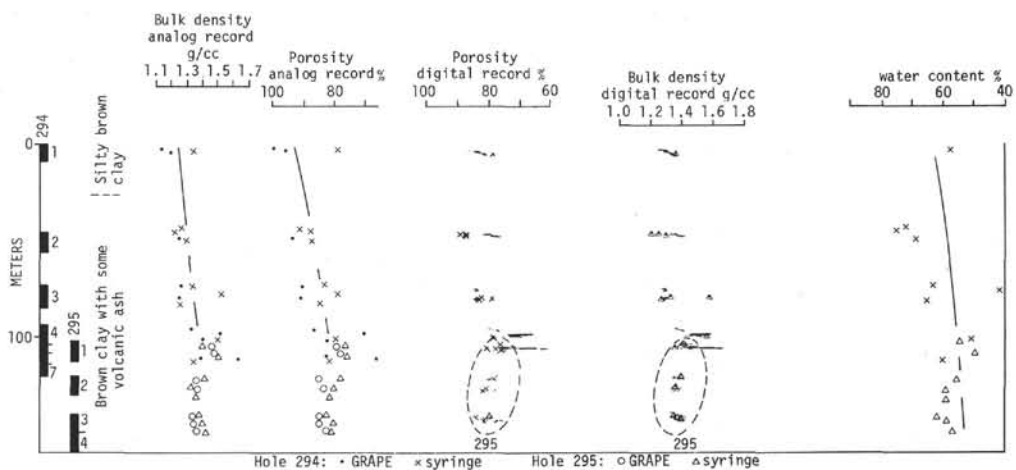


Figure 6. Plot of physical properties for Sites 294 and 295. GRAPE analog record readings as well as computer plot are presented in addition to laboratory analyses (syringe and chunk methods). On the left the cores are given as black rectangles and the general lithology.

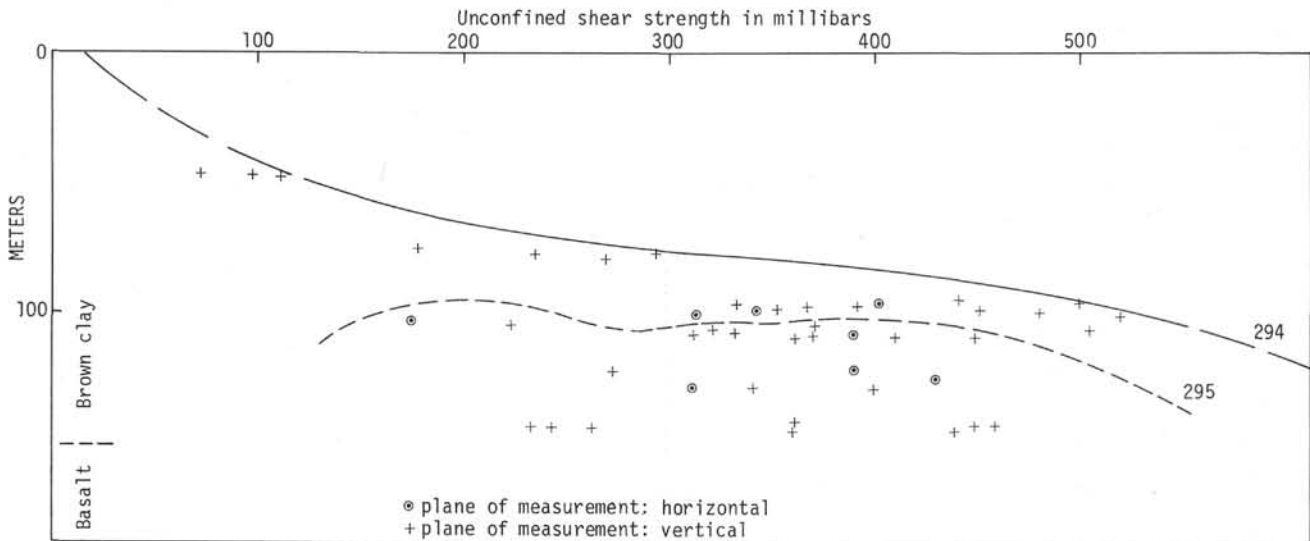


Figure 7. Plot of unconfined shear strength with depth, Sites 294 and 295. The dashed line separates the data from both sites.

TABLE 10
Vane Shear Data, Site 294

Sample (Interval in cm)	Depth (to nearest half meter)	Plane of Measurement	Shear Strength (mbar)
2-1, 136	53	Vertical	72.2
2-2, 35	54	Vertical	97.6
2-2, 120	55	Vertical	111.3
3-1, 140	77	Vertical	177.6
3-2, 110	79	Vertical	292.8
3-3, 40	79	Vertical	234.2
3-4, 90	81	Vertical	268.4
4-1, 135	94	Vertical	439.2
4-2, 100	96	Vertical	497.8
4-2, 150	96.5	Horizontal	400.2
4-3, 32	97	Vertical	331.8
4-3, 134	98	Vertical	366.0
4-4, 7	98	Vertical	390.4
4-4, 60	99	Vertical	351.4
4-4, 129	99.5	Vertical	449.0
4-4, 150	99.5	Horizontal	341.6
4-5, 45	100	Vertical	478.3
4-6, 0	101	Horizontal	312.32
4-6, 45	101	Vertical	517.3
6-1, 71	114	Vertical	502.6

TABLE 11
Vane Shear Data, Site 295

Sample (Interval in cm)	Depth (to nearest half meter)	Plane of Measurement	Shear Strength (mbar)
1-2, 0	104.5	Horizontal	175.7
1-2, 140	106	Vertical	370.9
1-3, 25	106	Vertical	224.5
1-3, 134	107.5	Vertical	322.1
1-4, 25	108	Vertical	390.4
1-4, 90	108.5	Vertical	331.8
1-4, 140	109	Vertical	370.9
1-5, 0	109	Horizontal	390.4
1-5, 50	109.5	Vertical	312.3
1-5, 98	110	Vertical	409.9
1-5, 100	110	Vertical ^r	449.0
1-5, 140	110.5	Vertical	361.1
1-5, 150	110.5	Vertical	390.4
2-2, 0	122.0	Horizontal	390.4
2-2, 59	122.5	Vertical	273.3
2-4, 0	125.0	Horizontal	429.4
2-6, 0	128.0	Horizontal	312.3
2-6, 34	128.0	Vertical	341.6
2-6, 125	129	Vertical	400.2
3-2, 38	154	Vertical	361.1
3-2, 111	154.5	Vertical	449.0
3-3, 45	155.5	Vertical	458.7
3-3, 120	156.0	Vertical	234.0
3-3, 130	156.0	Vertical	244.0
3-4, 0	156.5	Vertical	263.5
3-4, 37	157.0	Vertical	361.1
3-4, 70	157.0	Vertical	439.2
3-4, 130	158.0	Vertical	439.2

beds remain unconsolidated/unlithified throughout this lithological unit. Sand and silt beds, ranging in thickness up to 16 cm, occurred in 8 out of the 12 cores of this unit. Some were graded, others did not show such structure. Overturning of some beds could be established.

The analog records were very erratic due to the fissile nature of the material, and proper estimation of the density values may be slightly off. Many section curves were broken up into portions (Table 16) to provide better averages. When the record from a section was divided into two or three portions, a considerable difference in density resulted. Normally the middle portion had a much higher value than the top and bottom ones. This is thought to be due to fissility, creating more hair cracks the longer the material moves up during coring. In addition,

more expansion can occur on the top and bottom of a core under release of hydrostatic pressure.

When comparing the water-content data, a difference can be seen between the syringe sampling and the chunk method, the first one creating more voids when inserting the syringe. Scattering and a downward increase in density are absent as can be seen in Figure 12. On the contrary, a strong scattering in porosity data exists.

TABLE 12
Bulk Density, Porosity, and Water Content as Determined by the GRAPE and Syringe Methods, Site 296

Core	Section	Diameter (in.)	Interval (cm)		Lithology	GRAPE		Syringe		Remarks	
			GRAPE	Syringe		Bulk Density (g/cc)	Porosity (%)	Water Content (%)	Bulk Density (g/cc)		Porosity (%)
1	3	2.25	A	70	Foram-clay nanno ooze	1.57	70.8	46.15	1.52	70.03	
	4	2.25	A	144-150	Foram-clay nanno ooze			43.56	1.54	67.23	
2	2	2.65	50-150	110	Foram-clay nanno ooze	1.57	70.8	48.59	1.51	73.31	
	5			144-150	Foram-clay nanno ooze	1.54	72.7	40.73	1.59	64.71	
3	6			40	Foram-clay nanno ooze			42.54	1.63	69.40	D
	2	2.65	A		Foram-clay nanno ooze	1.64	66.2				
	3	2.65	A	110	Foram-clay nanno ooze	1.61	68.2	43.19	1.27	54.66	D
4	4	2.65	A		Foram-clay nanno ooze	1.63	66.8				
	2	2.65	A	110	Foram-clay nanno ooze	1.55	72.1	48.42	1.49	72.29	D
5	3	2.65	A		Foram-clay nanno ooze	1.57	70.8				
	4	2.65	A		Foram-clay nanno ooze	1.53	73.4				
	2	2.65	A		Foram-clay nanno ooze	1.57	70.8				
6	3			40	Foram-clay nanno ooze			42.94	1.57	67.20	
	4	2.65	A	144-150	Clayey nanno ooze			41.38	1.61	66.51	
	4	2.65	A		Clayey nanno ooze	1.63	66.8				
7	4	2.65	A	40	Foram-clay nanno ooze	1.64	66.2	42.31	1.58	66.66	
	5	2.65	A		Foram-clay nanno ooze	1.65	64.9				
8	2	2.65	A	40	Foram-clay nanno ooze	1.56	71.4	44.59	1.52	67.95	
	4	2.65	A		Clayey nanno ooze	1.59	69.5				
9	3	2.65	A	40	Clayey nanno ooze	1.63	66.8	42.67	1.54	65.63	
	4	2.56	A	110	Clayey nanno ooze	1.67	64.2	38.32	1.65	63.29	
10	2	2.65	0-50		Foram-clay nanno ooze	1.68	63.6				
	5	2.65	50-150	110	Foram-clay nanno ooze	1.63	66.8	41.53	1.61	66.69	
	3	2.65	A	110	Foram-clay nanno ooze	1.63	66.8	44.14	1.55	68.54	
11	3	2.65	A	40	Clay micarb nanno ooze	1.58	70.2	46.75	1.53	71.34	
	6	2.65	A	144-150	Clay micarb nanno ooze			41.36	1.61	66.46	
	4	2.65	A	40	Clayey nanno ooze	1.65	65.6	42.58	1.58	67.40	
12	3			110	Clayey nanno ooze			44.99	1.54	69.26	
	4	2.65	A		Clayey nanno ooze	1.59	69.5				
13	5	2.65	A	75	Clayey nanno ooze	1.64	66.2	42.56	1.56	66.23	
	2	2.65	AI		Clayey nanno ooze	1.64	66.2				
14	3	2.65	AI	40	Clayey nanno ooze	1.62	67.5	43.04	1.55	66.91	
	1	2.65	AI		Clayey nanno ooze	1.55	72.1				
15	5	2.65	AI	40	Clayey nanno ooze	1.57	70.8	54.89	1.39	76.54	
	2	2.65	A		Clayey nanno ooze	1.63	66.8				
	3			144-150	Clayey nanno ooze			41.89	1.56	65.54	
16	4	2.65	A		Clayey nanno ooze	1.68	63.6				
	3	2.65	A	40	Clayey nanno ooze	1.68	63.6	39.69	1.63	64.85	
17	5	2.65	A	40	Clayey nanno ooze	1.70	62.3	37.42	1.66	61.94	
	2	2.65	0-75		Clayey nanno ooze	1.69	62.9				
	5	2.65	75-150		Clayey nanno ooze	1.72	60.9				
18	2	2.65	AI	40	Clayey nanno ooze	1.73	60.3	37.58	1.65	61.96	
				110	Clayey nanno ooze			34.93	1.73	60.34	
				110	Clayey nanno ooze	1.73	60.3	38.34	1.51	57.90	

19	2	2.65	A	40	Clayey nanno ooze	1.63	66.8	42.21	1.54	64.92	
	5	2.65	A		Clayey nanno ooze	1.67	64.2				
20	2	2.65	0-75		Clayey nanno ooze	1.75	59.0				
			75-150		Clayey nanno ooze	1.55	72.1				
	3			144-150	Clayey nanno ooze			44.27	1.52	67.11	
				144-150	Clayey nanno ooze			48.72	1.46	70.94	
21	3	2.65	A		Clayey nanno ooze (chalky)	1.63	66.8				
22	3	2.65	AI		Clayey nanno ooze (chalky)	1.54	72.7				
	5	2.65	0-75		Clayey nanno ooze (chalky)	1.55	72.1				
		2.65	75-150		Clayey nanno ooze (chalky)	1.74	59.6				
23	2	2.65	0-75		Clayey nanno ooze	1.60	68.8				
		2.65	75-150		Clay nanno ooze-chalk	1.72	60.9				
24	3	2.65	A		Clay nanno ooze-chalk	1.71	61.6				
25	2	2.65	0-75		Clayey nanno ooze	1.58	70.2				
			75-150		Clayey nanno ooze-chalk	1.65	65.6				
	3			144-150	Clayey nanno ooze-chalk			34.19	1.69	57.89	
				144-150	Clayey nanno ooze-chalk			36.75	1.64	60.21	Chunk method
	4	2.65	A		Clayey nanno ooze-chalk	1.72	60.9				
26	3	2.65	A		Clayey nanno ooze-chalk	1.73	60.3				
	5	2.65	A		Clayey nanno ooze-chalk	1.74	59.6				
27	3	2.65	A		Clayey nanno ooze-chalk	1.70	62.3				
28	4	2.65	A		Clayey nanno ooze-chalk	1.66	64.9				
	5	2.65	A		Clayey nanno ooze-chalk	1.66	64.9				
29	2	2.65	AC		Clayey nanno ooze-chalk and ash	1.63	66.8				
	5	2.65	A		Clayey nanno chalk	1.70	62.3				
30	3	2.65	AC		Clayey rad nanno chalk	1.58	70.2				
	4			144-150	Clayey rad nanno chalk			36.31	1.65	59.76	Chunk method
	5	2.65	A		Clayey rad nanno chalk	1.72	60.9				
31	2	2.65	A		Clayey nanno chalk	1.72	60.9				
32	3	2.65	A		Clayey nanno chalk	1.74	59.6				
33	3	2.65	75		Clayey nanno chalk	1.73	60.3				
	4	2.65	AC		Clayey nanno chalk	1.70	62.3				
	5	2.65	AC	144-150	Clayey nanno chalk	1.79	56.4	29.33	1.77	51.89	Chunk method
36	3	2.65	AC		Clayey nanno chalk	1.72	60.9				
	5	2.65	AC		Clayey nanno chalk	1.75	59.0				
37	3	2.65	AC		Clayey nanno chalk	1.73	60.3				
	5	2.65	AC		Clayey nanno chalk	1.73	60.3				
38	3	2.65	AC		Clayey nanno chalk	1.70	62.3				
		2.65	50		Volc. ash	1.95	45.9				
39	3	2.65	AC		Clayey nanno chalk	1.59	69.5				Ash layers
	4	2.65	0-75		Clayey nanno chalk	1.63	66.8				Ash layers
		2.65	75-150		Clayey nanno chalk	1.66	64.9				Ash layers
40	1			143-150	Clay-ash-nanno chalk			35.01	1.63	57.22	Chunk method
	3	2.65	AC		Clay-ash-nanno chalk	1.69	62.9				
	4	2.65	AC		Clay-ash-nanno chalk	1.73	60.3				
41	3	2.65	AC		Clay-ash-nanno chalk	1.67	64.2				
45	2			144-150	Ash rich nanno chalk			34.44	1.68	58.00	Chunk method
46	3	2.65	AC		Ash rich nanno chalk	1.75	59.0				
52	1	2.4	Piece 3	144-150	Clay-ash-nanno chalk	1.79	56.4	32.29	1.74	56.33	Chunk method
		2.35	Piece 13		Clay-ash-nanno chalk	1.71	61.6				
56	6	2.34	AC		Lapilli tuff	2.09	36.8				

Note: A = average reading of a rather smooth GRAPE analog record. AI = average reading of an irregular GRAPE analog record. AC = average reading of an irregular GRAPE analog record from a core section consisting of chunks. D = doubtful value due to balance problems.

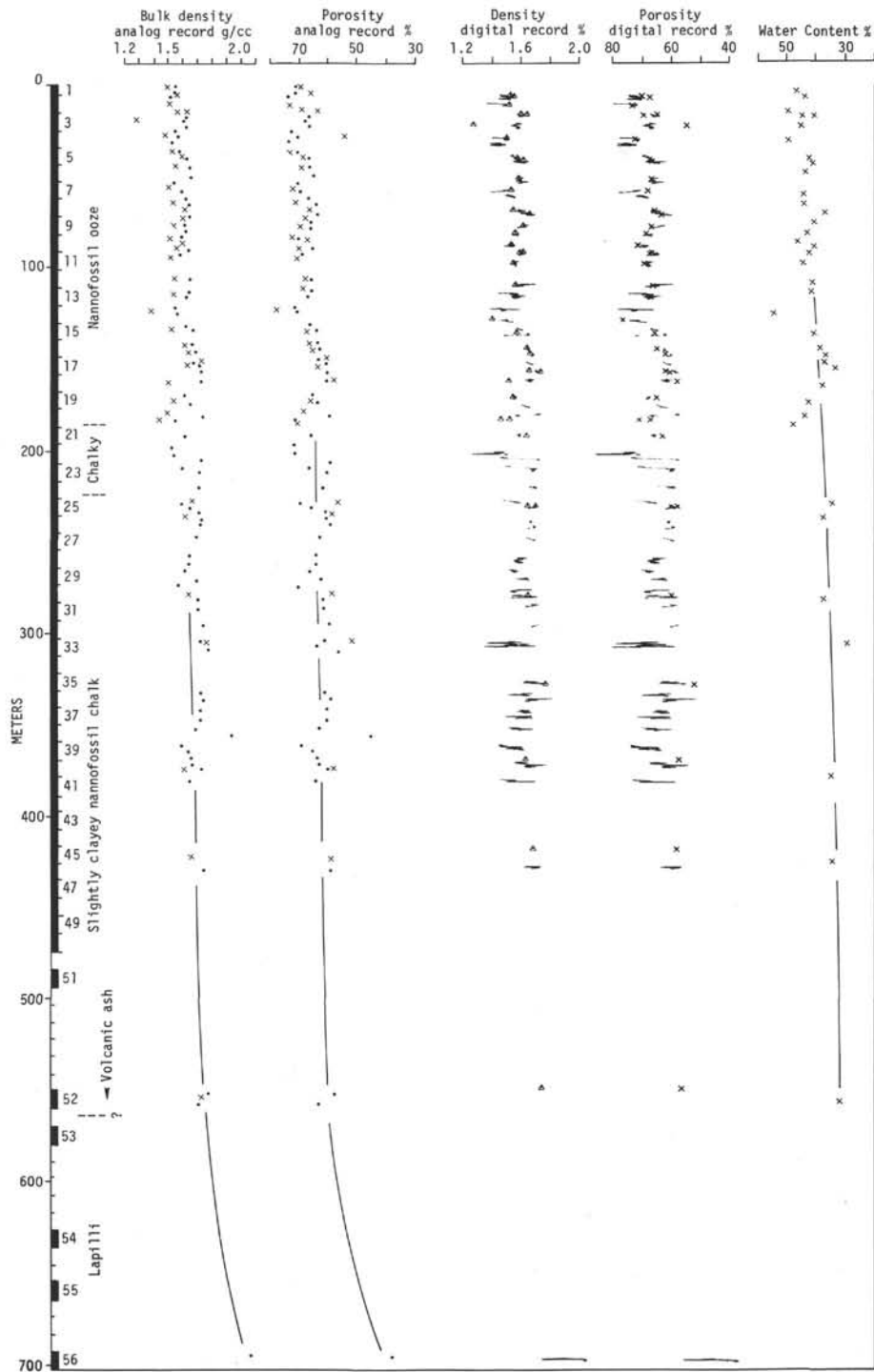


Figure 8. Plot of physical properties for Site 296. GRAPE analog record readings as well as computer plot are presented in addition to laboratory analyses (syringe and chunk methods). On the left the cores are given as black rectangles and the general lithology.

One piece of Core 10, Section 4, was measured on the GRAPE outside its liner. A bulk density of 1.83 g/cc and porosity of 53.8% were calculated using the 2.65 in. diameter. The actual diameter was 2.45 in. which boosts the density up to 1.98 g/cc, and the porosity then

becomes 43.9%. However, not all diameters were constant but a general increase of all values by 0.1-0.15 g/cc seems proper. This then places all laboratory values consistently lower than the GRAPE analog readings as has been normal for all other holes.

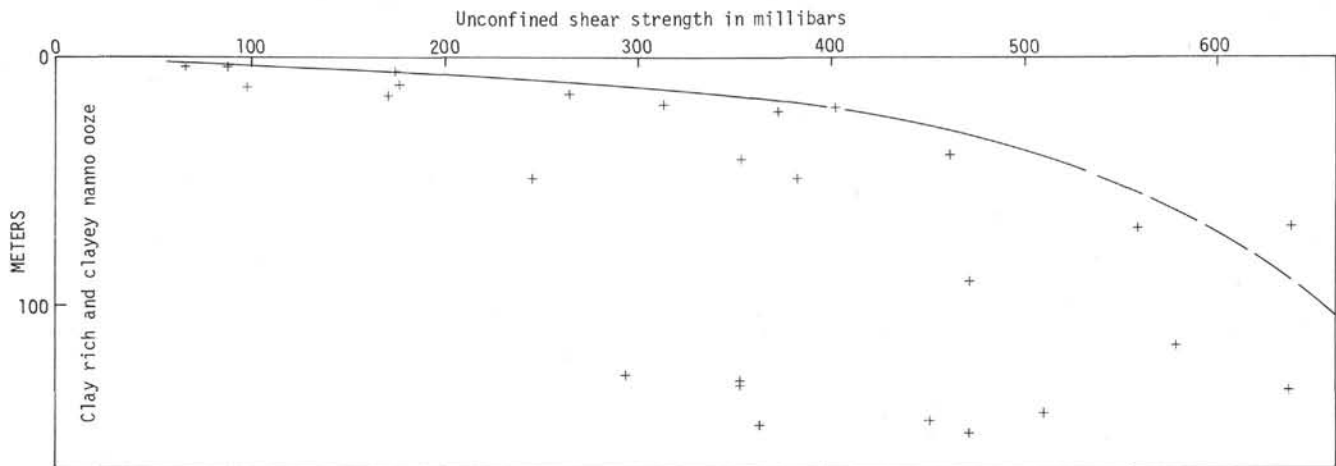


Figure 9. Plot of unconfined shear strength with depth, Site 296.

TABLE 13
Vane Shear Data, Site 296

Sample (Interval in cm)	Depth (to nearest half meter)	Plane of Measurement	Shear Strength (mbar)
1-2, 145	3.5	Vertical	66.4
1-3, 35	4.0	Vertical	87.8
1-4, 75	6.0	Vertical	173.7
2-3, 119	11.0	Vertical	175.7
2-4, 60	12.0	Vertical	97.6
2-6, 10	14.5	Vertical	263.5
2-6, 73	15.0	Vertical	169.8
3-2, 101	22.0	Vertical	312.3
3-3, 63	23.0	Vertical	400.2
3-4, 100	25.0	Vertical	370.8
5-3, 130	43.0	Vertical	458.7
5-4, 135	44.5	Vertical	351.4
6-3, 115	50.5	Vertical	380.6
6-4, 30	51.5	Vertical	244.0
8-4, 21	71.5	Vertical	634.4
8-4, 96	72.5	Vertical	556.3
10-6, 100	91.5	Vertical	468.9
13-4, 140	120.5	Vertical	575.8
14-6, 120	129.5	Vertical	292.8
15-3, 100	134.5	Vertical	351.4
15-2, 40	132.0	Vertical	351.4
15-4, 120	136.0	Vertical	634.4
16-4, 30	145.0	Vertical	507.5
16-6, 35	148.0	Vertical	449.0
17-1, 120	152.0	Vertical	361.1
17-3, 100	155.0	Vertical	468.9

In Figure 12 no corrections of the analog readings have been used. Most values for bulk density from the shaly unit of this site are already higher than those from similar depths of other holes or they correspond to the higher values. The main reason for not using a correction factor is that larger errors may be entered than the analog readings present due to unknown variations in fissility.

Vane Shear

The sparse vane-shear data in this large-scale overturned anticline, formed by underthrusting of the adjacent trench sediments, indicate low shear strength at

130 meters but a rapid increase through the interval from 130 to 180 m (Table 17, Figure 13). The low shear strength at 130 meters could be an artifact of drilling deformation, but consolidation tests indicate that the material is underconsolidated (Trabant et al., this volume). Although a sharp gradient of strengthening may be spurious, the water content from 130 to 180 meters shows a spectacular decrease suggesting that the shear-strength values indeed may be representative. The obvious remolding due to structural deformation makes it difficult to compare the sparse shear-strength data from Site 298 with similar information from other sites.

Site 299

This site was located in the submarine canyon fan complex of the Tayama Channel in the northwest corner of the Yamato Basin, Sea of Japan (see Bouma, this volume). No distinct lithological changes were found in this basically silty clay series in which some forams, diatoms, and volcanic ash are scattered or in thin layers. Some sand and clay layers were also present. Thirty-eight cores were drilled representing 532 meters of section. The two bottom cores are high in volcanic ash (Table 18, Figure 14).

The density values show a minor increase with depth. The gassy nature of the cores from the lower part of the hole may account for the low density values. The scattering is rather large due to the varying lithologies. Cores dominated by sand give relative high density values. The data obtained by the syringe-chunk methods generally show trends similar to values calculated from the GRAPE analog records.

Vane Shear

Vane shear determinations (Figure 15, Table 19) were made entirely in silty clays and clayey silts. The enveloping curve shows a concave downward shape indicating a decreasing rate of strengthening with depth.

Site 301

The location of this site was selected in such a way that it was furthest away from any of the major channels

TABLE 14
Bulk Density, Porosity, and Water Content as Determined by the GRAPE and Syringe Methods, Site 297

Core	Section	Diameter (in.)	Interval (cm)		Lithology	GRAPE		Syringe		Remarks			
			GRAPE	Syringe		Bulk Density (g/cc)	Porosity (%)	Water Content (%)	Bulk Density (g/cc)		Porosity (%)		
3	1	2.65	0-75	144-150	Diatom-ash-clay	1.48	76.7	53.66	1.41	75.60	Some ash		
	2		75-150		Diatom-rich clay							1.52	74.1
4	3	2.65	A	40	Diatom-ash-clay	1.49	76.1	43.41	1.58	68.74			
	2		A		Diatom-ash-clay							1.51	74.7
	5		0-75		Diatom-ash-clay							1.58	70.2
5	2	2.65	75-150	40	Diatom-ash-clay	1.60	68.8	44.89	1.54	69.27			
	4		A		Clay-rich nanno ooze							1.51	74.7
	5		A		Clay-rich nanno ooze							1.59	69.5
6	2	2.65	0-80	40	Clay-rich nanno ooze	1.52	74.1	41.40	1.56	64.60			
	4		80-150		Nanno-rich silty clay							1.54	72.7
	5		A		Nanno-rich silty clay							1.58	70.2
7	3	2.65	0-75	144-150	Nanno-rich silty clay	1.47	77.4	46.76	1.57	73.40			
	4		75-150		Clayey silt							1.63	66.8
	4		A		Clayey silt							1.58	70.2
8	3	2.65	A	40	Clayey silt	1.62	67.5	41.40	1.56	64.60			
	5		72-78		Volc. ash							1.80	55.7
	6		A		Nanno-rich clayey silt							1.62	67.5
9	2	2.65	A	33	Clayey silt	1.64	66.2	42.70	1.58	67.51			
	3		A		Clayey silt							1.62	67.5
	3		0-75		Clayey silt							1.55	72.1
10	3	2.65	75-150	144-150	Clayey silt	1.58	70.2	42.54	1.58	67.33			
	5		A		Clayey silt							1.58	70.2
	6		A		Clayey silt							1.58	70.2
11	2	2.65	0-75	29	Clayey silt	1.50	75.4	44.06	1.54	67.80			
	3		75-150		Clayey silt							1.58	70.2
	3		A		Clayey silt							1.58	70.2
12	4	2.65	A	144-150	Clayey silt	1.60	68.8	43.64	1.54	67.03			
	2		A		Clayey silt							1.64	66.2
	3		A		Clayey silt							1.62	67.5
13	1	2.65	0-75	112	Clay	1.77	57.7	44.54	1.52	67.49	Chunk method		
	2		75-150		Clay							1.82	54.4
	5		A		Clay							1.82	54.4
14	2	2.65	A	144-150	Clay	1.76	58.4	29.86	1.86	55.40			
	2		A		Clay							1.82	54.4
	4		0-120		Clay							1.82	54.4
15	2	2.65	120-160	35	Clayey sand	1.96	45.2	15.76	1.76	27.80			
	2		AI		Clay/silt-rich sand							2.10	36.1
	2		AI		Peat-rich ashey silt							2.10	36.1
16	2	2.65	0-50	144-150	Clay/silt-rich sand	2.12	34.8	14.51	2.08	30.23	AI		
	3		50-100		Sandy clay							2.05	39.3
	3		AI		Clay/silt-rich sand							2.05	39.3
17	1	2.65	AI	144-150	Clay/silt-rich sand	1.95	45.9	22.92	1.70	39.09			
	2		AI		Clay/silt-rich sand							1.95	45.9
	2		AI		Clay/silt-rich sand							1.95	45.9
18	2	2.65	AI	144-150	Clay	1.98	43.9	24.23	1.91	46.20	Chunk method		
	3		AI		Clay/silt-rich sand							1.98	43.9
	4		AI		Clay/silt-rich sand							1.98	43.9
19	3	2.65	AI	144-150	Clay	2.02	41.3	22.56	1.96	44.12	Chunk method		
	4		AI		Clay							1.99	43.7
	4		0-80		Clay/silt-rich sand							1.99	43.7
20	2	2.65	80-150	144-150	Clay	1.90	49.2	36.97	1.61	59.46	Chunk method		
	1		AI		Clay							1.90	49.2
	1		AI		Clay							1.90	49.2
21	3	2.65	AI	58	Volc. ash	1.65	65.6	28.94	1.68	48.75	Chunk method		
	4		A		Volc. ash							1.65	65.6
	6		A		Volc. ash							1.65	65.6
22	1	2.65	AI	4	Volc. ash with clay	1.65	65.6	23.43	1.91	44.69	Chunk method		
	1		AI		Volc. ash with clay							1.65	65.6

Note: A = average reading of a rather smooth GRAPE analog record. AI = average reading of an irregular GRAPE analog record.

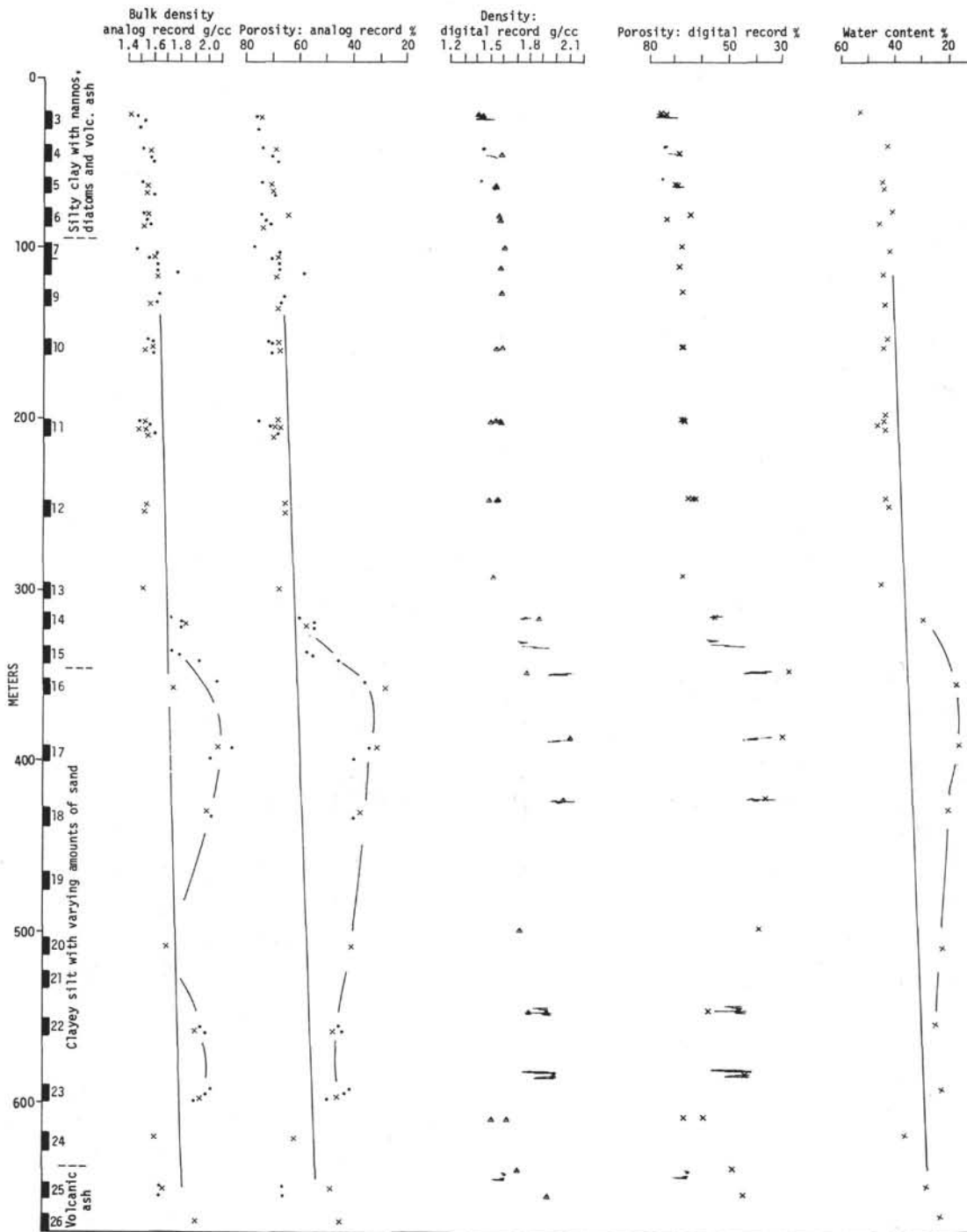


Figure 10. Plot of physical properties for Site 297. GRAPE analog record readings as well as computer plot are presented in addition to laboratory analyses (syringe and chunk methods). On the left the cores are given as black rectangles and the general lithology.

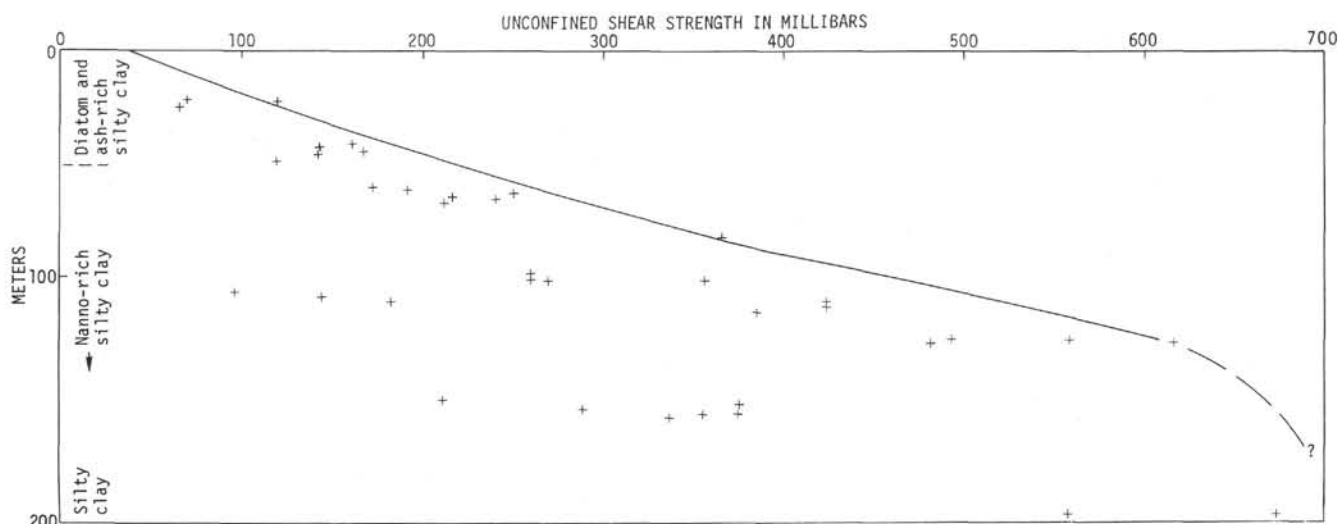


Figure 11. Plot of unconfined shear strength with depth, Site 297.

TABLE 15
Vane Shear Data, Site 297

Sample (Interval in cm)	Depth (to nearest half meter)	Plane of Measurement	Shear Strength (mbar)
3-1, 120	26.0	Vertical	68.8
3-2, 80	27.5	Vertical	118.5
3-3, 145	29.5	Vertical	65.0
4-1, 145	41.0	Vertical	160.6
4-2, 140	42.5	Vertical	141.5
4-3, 145	44.0	Vertical	166.4
4-4, 145	45.5	Vertical	141.5
4-6, 145	48.5	Vertical	118.5
5-1, 120	59.5	Vertical	171.1
5-2, 115	61.0	Vertical	191.2
5-3, 100	62.5	Vertical	248.6
5-4, 120	64.0	Vertical	215.1
5-5, 50	65.0	Vertical	239.0
5-6, 95	67.0	Vertical	210.3
6-4, 29	83.0	Vertical	363.3
7-2, 77	102.0	Vertical	258.1
7-3, 120	103.0	Vertical	353.7
7-3, 132	104.0	Vertical	258.1
7-4, 75	105.0	Vertical	267.7
8-1, 80	107.0	Vertical	95.6
8-2, 145	109.0	Vertical	143.4
8-3, 138	110.5	Vertical	181.6
8-4, 6	110.5	Vertical	420.6
8-5, 76	113.0	Vertical	420.6
8-6, 145	115.0	Vertical	382.4
9-1, 138	131.0	Vertical	489.6
9-2, 70	132.0	Vertical	554.5
9-2, 146	132.5	Vertical	611.8
9-3, 5	132.5	Vertical	478.0
10-1, 26	153.0	Vertical	210.3
10-2, 71	154.5	Vertical	372.8
10-3, 142	157.0	Vertical	286.8
10-4, 135	161.0	Vertical	353.7
10-5, 6	161.0	Vertical	372.8
10-6, 48	161.5	Vertical	334.6
11-3, 41	207.5	Vertical	554.5
11-3, 67	207.5	Vertical	669.2

feeding the abyssal plain. Twenty cores were taken over a 497-meter interval. The upper 7 cores, representing 240.5 meters of sediment column, contained primarily silty clays and clays. Minor interbeddings of sandy silts, silty sands, clayey sands, sands, and volcanic ash were encountered. Diatoms, radiolarians, sponge spicules, and silicoflagellates were common minor constituents. Below this unit a clayey diatomite, grading into a diatomaceous claystone, was found. Clay-mineral content varies from 30% to 54% and diatomite content from 30% to 50%.

Presence of gas was normal in most of the cores, resulting in many large and small expansion cracks making it difficult to carry out physical-property measurements. Syringe samples without cracks could not be collected at all except for the upper cores.

Most core sections had a slight difference between top and bottom density values. Very often the middle section was too broken up to obtain any rational curve at all (Table 20). Consequently, a large scattering of plotted data is to be expected (Figure 16). Using the limited number of data points and eliminating the higher values in Core 5, a minor downhole increase in density results.

Although the GRAPE values are doubtful, the syringe and chunk analyses are considered highly inaccurate. This becomes very obvious when viewing the water-content plots.

Site 302

This last hole of Leg 31 was drilled in 2399 meters of water on the Yamato Rise. A total of 18 cores was drilled representing 531.5 meters of section. The sediments were diatomaceous, except for both bottom cores. Lithologic variations enabled the shipboard sedimentologists to distinguish five units which is more detailed than that used for physical property studies. Core 18 consisted of volcanogenic material representing late Miocene volcanic activity which stratigraphically was followed by continuous pelagic sedimentation.

TABLE 16
Bulk Density, Porosity, and Water Content as Determined by the GRAPE and Syringe Methods, Site 298

Core	Section	Diameter (in.)	Interval (cm)		Lithology	GRAPE		Syringe		Remarks	
			GRAPE	Syringe		Bulk Density (g/cc)	Porosity (%)	Water Content (%)	Bulk Density (g/cc)		Porosity (%)
2	3	2.65	0-50	20	Clayey silt	1.52	74.1	45.90	1.51	69.46	
		2.65	50-70		Sand	1.90	49.2				
		2.65	70-150	135-150	Sandy clayey silt	1.53	73.4	44.51	1.55	68.77	
4	2	2.65	AI	60	Clayey silt	1.80	55.7	30.87	1.73	53.40	Chunk method ^a
				144-150	Clayey silt			23.19	1.97	45.60	
	3	2.65	AI		Clayey silt	1.78	57.0				Silty, sandy
5	2	2.65	AI	110	Silt-rich clayey sand	1.85	52.5	21.67	1.82	39.55	Chunk method ^a
6	1			144-150	Silt-rich claystone			25.53	1.69	43.03	
	2	2.65	0-50		Silt-rich claystone	1.80	55.7				
		2.65	50-100	93-94	Silt-rich claystone	1.94	46.6	24.14	1.71	41.18	Chunk method ^a
		2.65	100-150		Silt-rich claystone	1.77	57.7				
7	1			144-150	Shale			20.95	1.62	33.91	
	2	2.65	AI	14	Clayey shale	1.84	53.1	24.07	1.86	44.83	Chunk method ^a
8	1			133-135	Shale			24.03	1.82	43.81	Chunk method ^a
	2	2.65	0-75		Shale	1.59	69.5				
		2.65	75-150		Shale	1.79	56.4				
9	1	2.65	AI	144-150	Ash-rich shale	1.73	60.3	23.76	1.78	42.36	Chunk method ^a
10	2	2.65	A		Shale	1.85	52.5				
11	3			15-16	Shale			21.19	1.93	40.85	Chunk method ^a
				144-150	Shale			23.65	1.83	43.19	Chunk method ^a
12	2	2.65	AI		Shale	1.80	55.7				
	3	2.65	AI		Shale	1.84	53.1				
	4	2.65	0-75		Shale	1.75	59.0				
		2.65	75-150		Shale	1.81	55.1				
	5	2.65	AI		Shale	1.84	53.1				Sandy
13	2	2.65	AI		Silty shale	1.83	53.8				
	3	2.65	A	40	Silty shale	1.85	52.5	21.13	1.82	38.46	Chunk method ^a
				120	Silty shale			20.59	1.84	37.84	Chunk method ^a
	4	2.65	0-100		Silty shale	1.83	53.8				
		2.65	100-150	144-150	Silty shale (sandy)	1.90	49.2	22.01	1.91	42.00	Chunk method ^a
	5	2.65	AI	30	Silty shale	1.86	51.8	22.71	1.82	41.40	Chunk method ^a
14	2	2.65	AI	108-109	Silty shale	1.87	51.1	20.39	1.87	38.18	Chunk method ^a
	3	2.65	0-100		Silty shale	1.78	57.0				
		2.65	100-150	144-150	Silty shale (sandy)	1.83	53.8	20.89	1.93	40.27	Chunk method ^a
	4	2.65	AI		Silty shale	1.87	51.1				
15	3	2.65	A	144-150	Silty shale	1.88	50.5	19.32	1.99	38.42	Chunk method ^a
	5	2.65	A	80-82	Silty shale	1.90	49.2	20.15	1.95	39.26	Chunk method ^a
16	2			130-132	Silty shale			18.46	1.84	34.04	Chunk method
				144-150	Silty shale			17.06	2.05	34.93	Chunk method
	3	2.65	0-75		Silty shale	1.86	51.8				
			75-150		Silty shale	1.89	49.8				
	4	2.65	AI		Silty shale	1.92	47.9				
	5	2.65	AI		Silty shale	1.92	47.9				

Note: A = average reading of a rather smooth GRAPE analog record. AI = average reading of an irregular GRAPE analog record.

^ameasurement may not be too accurate due to crumbly nature of samples resulting in possible loss of some small pieces during the analysis.

Variations in the type and amount of this type of deposition are reflected in the sediments.

From Cores 2 through 5 a minor downhole increase in density, coupled with medium scattering, can be observed (Table 21, Figure 17). This is followed by almost constant density, porosity, and water-content values through Core 14. The zone of nearly constant values distinguishes itself from the top five cores by minimum scattering.

The diatomites have low bulk-density values and indicate the trend the physical properties follow below Core 14. Two pieces from Core 17, Section 2, were measured outside the liner, presenting values for density of 1.55 and 1.51 g/cc. By using the actual diameters, 2.35 and 2.37 in., respectively, the density values become 1.37 and 1.35 g/cc. This places their plots straight in line with those of the overlying unit.

In the zone where there are nearly constant values with depth, very little scattering occurs and values are lower than others obtained during Leg 31. The values place these diatomaceous oozes in a category apart. Consolidation may take place initially, but overburden seems to have no effect (Trabant et al., this volume). In Figure 17 two mean lines are given, one for the upper five cores and one for the underlying ones.

Vane Shear

The Site 302 shear-strength data also show two trends (Figure 18, Table 22). Down to 80 meters the shear strength increases rapidly with depth; whereas, below this depth there is both a marked decrease in absolute strength and a decrease in the rate of increase of shear strength. This sharp discontinuity is apparently due to a transition from a predominantly clayey lithology to a

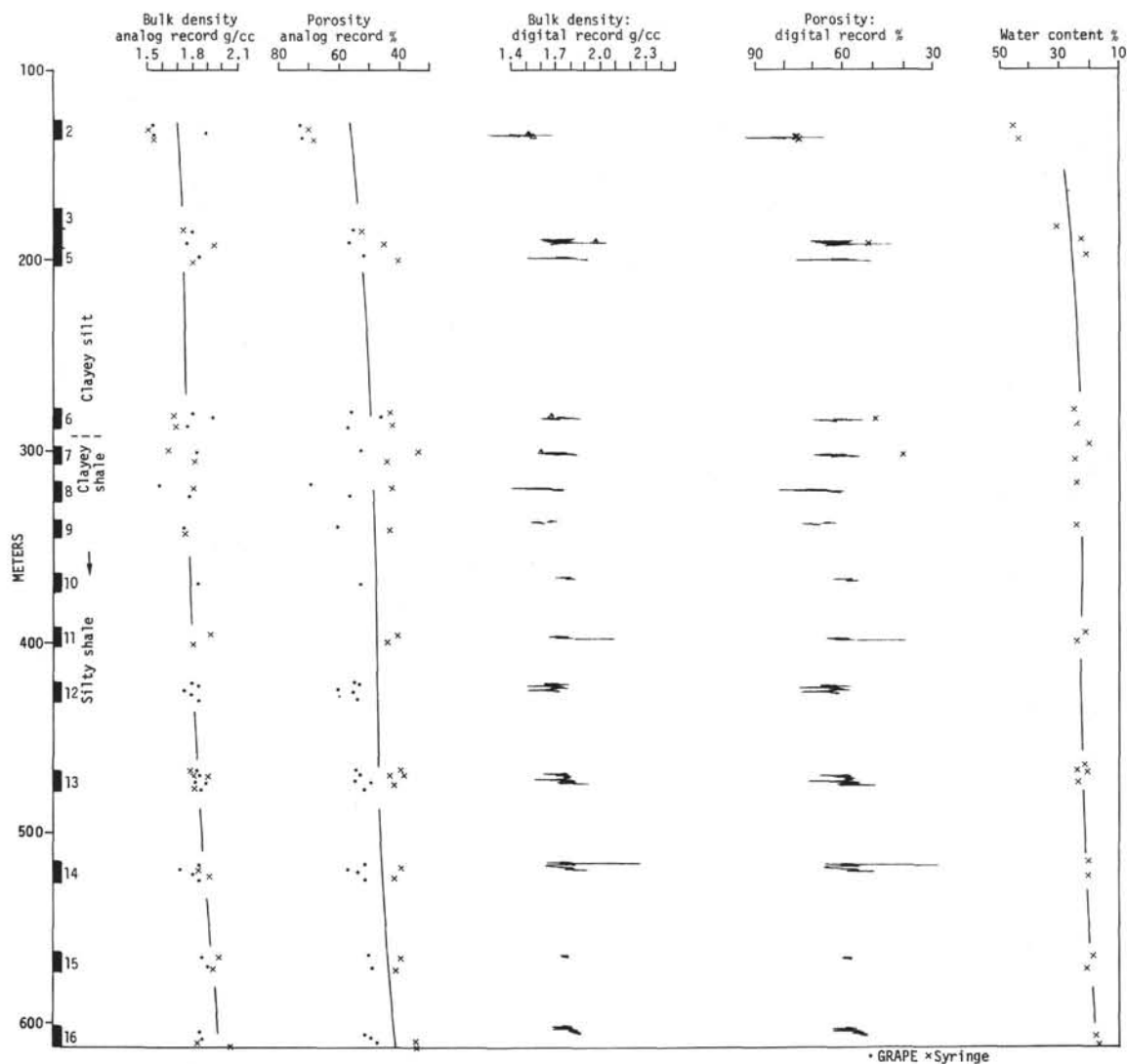


Figure 12. Plot of physical properties for Site 298. GRAPE analog record readings as well as computer plot are presented in addition to laboratory analyses (syringe and chunk methods). On the left the cores are given in black rectangles and the general lithology.

diatom ooze. This decrease in shear strength also corresponds with an increase of porosity from about 75% to 80% (water content similarly changes from less than 50% to more than 55%).

CONCLUSIONS

The GRAPE measurements as well as the syringe/chunk methods are routinely performed often without a geotechnically trained scientist involved. As a result the data collected can only be used to identify overall trends rather than for specifics. Most of the flaws in the techniques have been extensively discussed by Bennett and Keller (1973). Coring distortion is the most serious source of errors with regard to GRAPE measurements. Generally, a decrease in the degree of disturbance can be observed downward in each core due to the distance over which material has moved up into the core barrel as well as the time it was subjected to drilling vibration. Once the sediment becomes more

consolidated these effects decrease in magnitude. Consequently, the lowest sections should be measured only or, if more sections were measured, their results should be disregarded or handled very carefully based on disturbance observations from split sections. Also more notice should be given to breaks and water pockets in the core sections, and frequent measurements should be made on the diameter of the core section. These factors account for a large amount of the scattering. In addition, one deals with drift in the GRAPE unit.

Weighing onboard ship can introduce large errors which add considerably to the inaccuracies in 1-cc syringe sample collection (see also Bennett and Keller, 1973). Inserting the syringe often creates hair cracks which can significantly influence the small volume.

Bulk Density Versus Lithology

Although bulk densities are well known for different types of materials, the combination of instrument drift,

TABLE 17
Vane Shear Data, Site 298

Sample (Interval in cm)	Depth (to nearest half meter)	Plane of Measurement	Shear Strength (mbar)
2-2, 47	132.5	Vertical	23.4
2-2, 83	132.5	Vertical	37.1
2-2, 137	133	Vertical	23.4
2-3, 48	134	Vertical	25.4
2-3, 90	134.5	Vertical	33.2
2-4, 128	136	Vertical	27.3
2-4, 145	136	Vertical	23.4
4-1, 52	189.5	Vertical	415.0
4-1, 138	190	Vertical	268.5
4-1, 138	190	Vertical	439.4
4-2, 38	191	Vertical	512.6
4-2, 89	191.5	Vertical	585.9
4-2, 138	192	Vertical	488.2
4-3, 105	193	Vertical	549.3
5-2, 27	202	Vertical	585.9
5-2, 37	202	Vertical	488.2
6, CC	288	Horizontal	341.7
6, CC	288	Horizontal	439.4
6, CC	288	Horizontal	366.2
6, CC	288	Horizontal	659.1

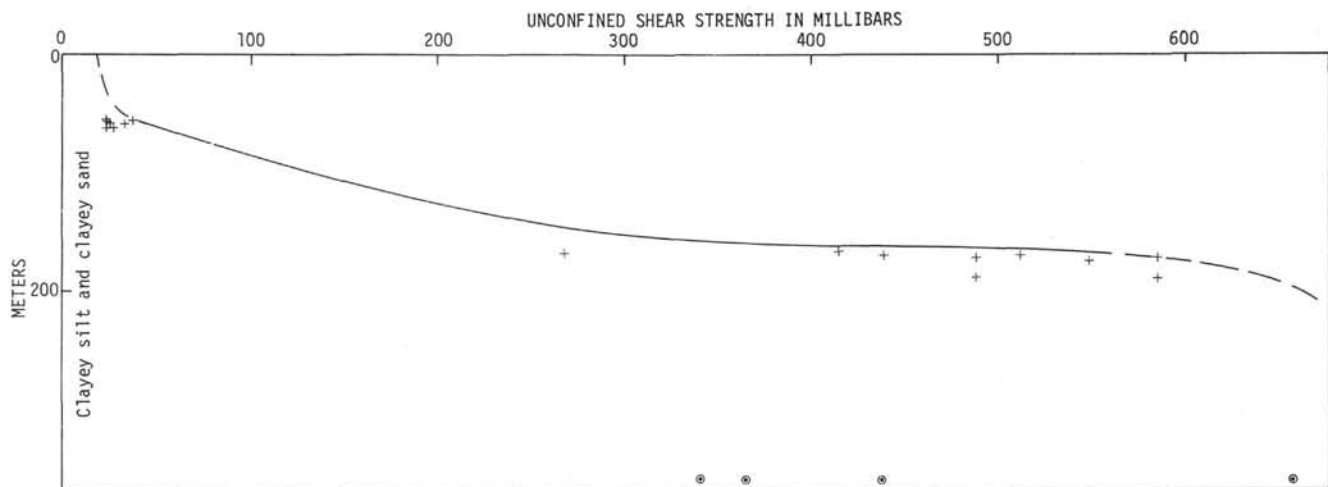


Figure 13. Plot of unconfined shear strength with depth, Site 298.

scattering due to sediment variations, and scattering based on artificial influences results in plots which do not reveal lithology. Figure 19 presents compilations of two sets of lithology groups with depth. One plot is made from all bulk density plots presented earlier per site where sediments were encountered that consist of any mixture of sand, silt, and clay as major constituents. It was found impossible to select accurately single lithologies due to insufficient size analyses. Such single lithology plots only become realistic if the degree of distortion is added. In Figure 19 the GRAPE analog readings are combined with the syringe/chunk data which accounts for even more scattering. A mean drawn through this plot presents a rather linear increase downward from about 1.4 g/cc at the top to 1.84 g/cc at the bottom. If diameters of the cores had been known better (see Test Results) and data from highly distorted sections eliminated, one would observe more parallel

trends between various lithologies. The Site 298 plots would have been positioned at the outer right-hand side of the total plot and the Site 294/295 ones more on the left.

The other set of data points in Figure 19 is based on nannoplankton ooze/chalk with varying amounts of other components and on diatom ooze. The latter clearly has a lower density than the nannofossil series and displays a smaller increase in density with depth. A mean line for the diatom ooze is nearly vertical representing a value of 1.35 g/cc. Such a line for the nannofossil series starts at zero depth at about 1.55 g/cc and may become as high as 2.09 g/cc at 620 meters depth. If this is true the three points at Site 296 at about 545 meters depth are too low in value.

In general, it can be concluded that the bulk density, porosity, and water-content data are not accurate enough to draw precise conclusions.

TABLE 18
Bulk Density, Porosity, and Water Content as Determined by the GRAPE and Syringe Methods, Site 299

Core	Section	Diameter (in.)	Interval (cm)			GRAPE		Syringe		Remarks	
			GRAPE ^a	Syringe		Bulk Density (g/cc)	Porosity (%)	Water Content (%)	Bulk Density (g/cc)		Porosity (%)
1	4			100	Silty clay			54.99	1.41	77.60	
	5			144-150	Silty clay			57.10	1.40	80.03	
2	4	2.65	A	100	Foram-rich silty clay	1.54	73	50.49	1.46	73.63	
3	4	2.65	A		Silty clay	1.53	73.5				
4	4	2.65	0-60		Foram-diatom-clay ooze	1.50	75				
		2.65	60-115	115	Silty clay	1.55	72	53.66	1.40	74.97	
5	2	2.65	0-95	67	Silty clay	1.48	77	44.21	1.58	69.83	
		2.65	95-150		Foram-diatom silty clay	1.52	74				
6	5	2.65	A	45	Sandy silty clay	1.54	73	42.76	1.58	67.49	
7	3	2.65	A	111	Silty clay	1.53	73.5	49.30	1.46	71.94	
8	3	2.65	A	127	Silty clay	1.53	73.5	50.44	1.46	73.86	Volc. ash
9	5	2.65	0-60		Silty clay	1.53	73.5				
		2.65	60-150		Silty sand	1.76	58				
10	4			144-150	Silty clay			51.59	1.45	74.60	
	5	2.65	0-75		Sandy silty clay	1.48	77				
		2.65	75-150	100	Sandy silty clay	1.60	68	48.95	1.47	72.10	Less sandy
11	5	2.65	A		Silty clay	1.48	77				
12	5	2.65	0-110		Silty clay	1.55	72				
		2.65	110-150		Sandy	1.75	59				
13	3	2.65	A		Clayey silt	1.48	77				
	5	2.65	A		Silty clay	1.50	75				
14	4	2.65	0-100		Sandy silty clay	1.55	72				
		2.65	100-150		Clayey silty sand	1.69	63				
15	2	2.65	A		Clayey silt	1.48	77				
	4			144-150	Clay			39.16	1.63	63.69	
16	3	2.65	A	15	Silty clay	1.61	68	41.37	1.55	64.26	
17	2	2.65	0-40		Sandy silty clay	1.76	58				
		2.65	60-100		Silty clay	1.61	68				
		2.65	100-150		Sandy silt	1.80	56				
18	4	2.65	0-75		Clay	1.55	72				
		2.65	75-120		Silty clay	1.48	77				
		2.65	120-150		Sandy silty clay	1.62	68				
19	5	2.65	A		Sandy silty clay	1.73	60				
20	2	2.65	0-120		Silty clay	1.62	68				
		2.65	120-150	144-150	Sandy	1.71	61	33.71	1.71	57.74	
22	3	2.65	A		Silty clay	1.54	73				
	4	2.65	A		Silty clay	1.49	76				
29	1	2.65	-		Sandy silty clay	1.60	68				
30	4	2.65	A	144-150	Silty clay	1.60	68	38.75			
31	2	2.65	A		Silty clay	1.58	70				
32	1			144-150	Micarb-rich silty clay			34.20			
	2	2.65	A		Micarb-rich silty clay	1.69	63				
33	2	2.65	A		Silty clay	1.60	68				
35	2	2.65	0-70		Silty clay	1.53	73.5				
36	2			144-150	Slightly silty clay			28.27			
	4	2.65	A		Ash-rich silty clay	1.84	53				Layered
37	2	2.65	A		Ash-rich silty clay	1.82	54				Layered
	3	2.65	A		Ash-rich silty clay	1.90	49				Layered

^aA = average reading from the GRAPE analog record.

Horizontal Versus Vertical Shear Strength

Most vane-shear measurements were made on core faces, whereas a few were made on horizontal bedding surfaces. The shear-strength measurements taken in the vertical plane are generally higher than the adjacent horizontal determinations (see Figure 7 and Tables 7, 10, 11, 17, and 20). This discrepancy can be accounted for by the fact that vertical measurements were taken across bedding anisotropy, but the horizontal measurements were made in the bedding plane which probably has a nearly isotropic fabric.

Shear Strength Versus Lithology

One of the most significant results of the shear-strength studies on Leg 31 was the opportunity to compare consistently determined strength profiles for a wide variety of deep-sea sediments. The enveloping curves of the uncorrected shear-strength data are summarized in Figure 20. In Figure 21 the various enveloping curves are identified by lithology: carbonate ooze (Site 299); pelagic brown clay (Site 294); diatom ooze (Site 302, lower portion); hemipelagic-terrigenous mud (average of Sites 297, 299, 302 [upper portion]). Results from Site

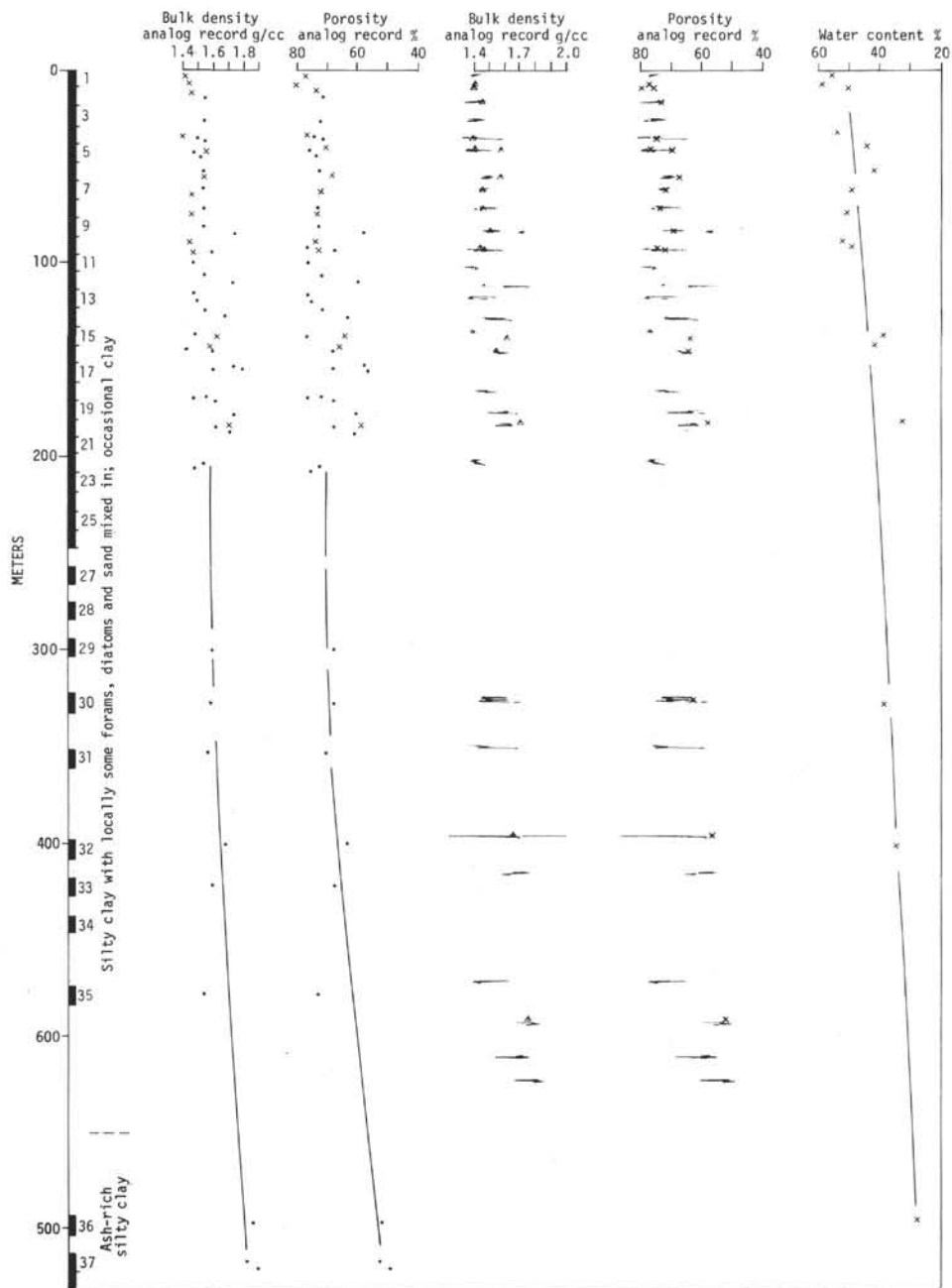


Figure 14. Plot of physical properties for Site 299. GRAPE analog record readings as well as computer plot are presented in addition to laboratory analyses (syringe and chunk methods). On the left the cores are given as black rectangles and the general lithology.

298 are not utilized in the following comparison since they show postdepositional structural disturbance.

In order to better compare shear strengths of various lithologies, the values and percentage differences for 50 and 100 meters have been compiled (Table 23). At 50 meters the pelagic brown clay is the weakest lithology, the hemipelagic-terrigenous mud is of medium strength and the carbonate ooze is by far the strongest. At 100 meters the relative differences in strength have markedly decreased. The carbonate ooze has the strongest lithology; the hemipelagic-terrigenous mud and brown

pelagic clays are weaker, but of comparable strength; the diatom ooze is the weakest sediment at 100 meters.

The higher strength of the carbonate ooze is probably due to incipient cementation which would increase the cohesion of the sediment over and above that caused by compaction and dewatering. In support of this interpretation, Roth and Thierstein (1972) have noted slight degrees of secondary calcite overgrowth on particles in carbonate oozes buried approximately 100 meters. The weakness of diatomaceous deposits relative to clayey sediments has been previously noted in cores recovered

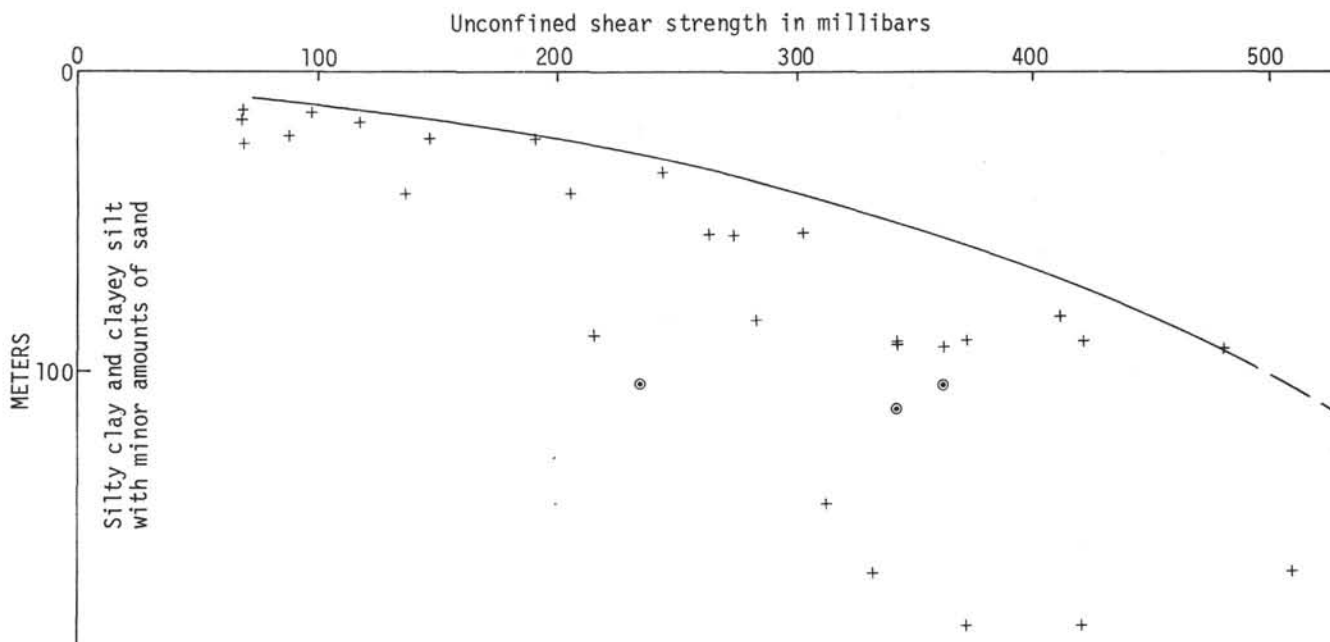


Figure 15. Plot of unconfined shear strength with depth, Site 299.

TABLE 19
Vane Shear Data, Site 299

Sample (Interval in cm)	Depth (to nearest half meter)	Plane of Measurement	Shear Strength (mbar)
2-3, 57	15	Vertical	68.4
2-3, 91	15.5	Vertical	97.7
2-5, 52	18	Vertical	67.9
2-5, 131	19	Vertical	117.7
3-2, 75	25	Vertical	87.9
3-2, 144	25.5	Vertical	190.4
3-3, 17	25.5	Vertical	146.5
3-4, 68	27.5	Vertical	68.4
4-4, 43	37	Vertical	244.1
5-2, 78	42.5	Vertical	136.7
5-2, 87	42.5	Vertical	205.1
5-2, 123	43.0	Vertical	136.7
6-5, 10	55.5	Vertical	302.7
6-5, 60	56.0	Vertical	263.6
6-5, 104	56.5	Vertical	273.4
9-4, 75	83.5	Vertical	410.1
9-5, 41	89.5	Vertical	283.2
10-2, 111	90.0	Vertical	214.8
10-3, 95	91.5	Vertical	371.1
10-3, 103	91.5	Vertical	419.9
10-4, 20	92.0	Vertical	341.8
10-4, 120	93.0	Vertical	341.8
10-5, 38	94.0	Vertical	361.3
10-5, 95	94.5	Vertical	478.5
11, CC	104.5	Horizontal	234.4
11, CC	104.5	Horizontal	361.3
12, CC	114.0	Horizontal	341.8
16-2, 10	147.5	Vertical	312.5
18-4, 30	170.0	Vertical	507.8
18-4, 97	170.5	Vertical	332.0
20-3, 108	189.5	Vertical	419.9
20-3, 112	189.5	Vertical	371.1

from the Bering Sea (Lee, 1973). Lee's consolidation experiments show that diatom oozes are markedly less compressible than clayey sediments at low to moderate stresses. Therefore, the relative increase in the number and extent of grain-to-grain contacts is less within a diatom ooze than in clayey sediment and the cohesion (shear strength) of the diatom ooze increases slowly during shallow burial.

The convergence in shear strength between the pelagic brown clay and hemipelagic-terrigenous mud may be due to the rapid decrease in water content (and porosity) of former lithology. For example, the water content of the pelagic brown clay (Site 294) decreases from 71% to 51% over the interval from 50 to 100 meters whereas the water content of the hemipelagic-terrigenous mud (average of Sites 297 and 299) drops only from 47% to 43.5% over the same interval. The initial high water content of the pelagic brown clay is undoubtedly due to its fine uniform grain size.

These physical or geotechnical properties, except the vane shear, are measured as a routine procedure onboard *Glomar Challenger*. However, on most legs no experts are present and the sedimentologist(s) and/or geophysicist(s) have to take responsibility for this aspect of the program in addition to his normal duties. As a result, the data from many legs are not comparable and the field of marine geotechnique, which is still in its infant stage, suffers from this great opportunity the Deep Sea Drilling Program can offer.

RECOMMENDATIONS

The routine of the GRAPE measurements should be changed. The marine technicians are instructed to

TABLE 20
Bulk Density, Porosity, and Water Content as Determined by the GRAPE and Syringe Methods, Site 301

Core	Section	Diameter (in.)	Interval (cm)		Lithology	GRAPE		Syringe		Remarks	
			GRAPE ^a	Syringe		Bulk Density (g/cc)	Porosity (%)	Water Content (%)	Bulk Density (g/cc)		Porosity (%)
2	2	2.65	0-130	144-150	Silty clay	1.46	78	51.12	1.45	74.09	
		2.65	130-150		Sandy silty clay	1.53	73				
3	3	2.65	0-100	144-150	Silty clay	1.45	79	20.62	1.71	35.23	
		2.65	100-150		Silty clay with ash	1.52	74				
	2.65	0-50	Silty clay		1.51	74.7					
	2.65	50-120	Sand		1.60	69					
4	3	2.65	120-150	144-150	Silty clay	1.51	74.7	48.17	1.45	69.89	Gas voids
		2.65	120-150		Silty clay	1.51	74.7				
5	6	2.65	30-100	144-150	Sandy silty clay	1.70	62	41.29	1.53	63.10	Gas voids
		2.65	100-150		Clay	1.75	59				
8	2	2.65	144-150	144-150	Clay	1.75	59	45.67	1.49	67.94	Gas voids
		2.65	144-150		Clayey diatom ooze	1.52	74				
11	1	2.65	144-150	144-150	Clayey diatomite	1.60	69	47.92	1.37	65.80	Chunk method
15	3	2.65	144-150	144-150	Clayey diatomite	1.58	70				
18	2	2.65	0-45	144-150	Clayey diatomite	1.60	69	25.45	1.83	47.06	Gas voids
		2.65	95-150		Clayey diatomite	1.60	69				
	2.65	0-95	Clay		1.58	70					
	2.65	95-130	Sandy silty clay		1.70	62					
19	3	2.65	144-150	144-150	Clay	1.70	62	25.73	1.83	47.06	Gas voids
		2.65	144-150		Clay	1.70	62				
19	5	2.65	AI	144-150	Diatomaceous claystone	1.65	66	39.71	1.55	61.49	Gas voids
		2.65	0-50		Micarb claystone	1.54	73				
20	3	2.65	100-150	144-150	Micarb claystone	1.60	69	37.00	1.61	61.01	Gas voids
		2.65	0-60		Diatomaceous claystone	1.65	66				
	2.65	70-130	Diatomaceous claystone		1.60	69					
	2.65	144-150	Diatomaceous claystone		1.60	69					
20	4	2.65	144-150	144-150	Diatomaceous claystone	1.60	69	37.98	1.61	61.01	Gas voids
		2.65	144-150		Diatomaceous claystone	1.60	69				
20	4	2.65	144-150	144-150	Diatomaceous claystone	1.60	69	37.98	1.61	61.01	Gas voids
		2.65	144-150		Diatomaceous claystone	1.60	69				

Note: Most analog records have irregular curves due to gas voids. AI = average reading of a very irregular GRAPE analog record.

^aSyringe sample taken from softer disturbed sediment near plastic liner; chunk from hard center.

^bVolume slightly off due to small voids in sample.

measure at least two sections per core, normally the numbers 2 and 5. Little attention is paid to the degree of visible disturbance of the uncut core. The scientists in charge should select which sections are to be measured, preferably at least always the lowest section. In addition to disturbance, measurements should be done on the diameter of each measured section and the thickness of the liner. Too often this diameter is assumed to be 2.60 in. (6.6 cm) for normal cores and 2.25 in. (5.71 cm) for punch cores. It is recommended to measure less core sections and to spend more time on each measurement. The scientist in charge should have a good updated set of instructions available instead of sets of instructions of different dates. He should make a list of each section measured with regard to dimensions, lithology, filling of the liner, and degree of distortion. Also some quantitative notes about each analog record should be made. This scientist also should select the location for taking cylinder samples and larger syringe samples.

Utilization of the "Torvane" apparatus on Leg 31 has shown that it is a viable instrument for rapid determination of unconfined shear strength on split core faces. In addition to estimates of consolidation and lithification, vane-shear measurements provide a rapid means of quantitatively estimating core disturbance within a given lithology. In view of the small variation of vane-shear strength values between lithologies, routine collection of vane-shear data on successive DSDP cruises is recommended. It is expected that consistent

patterns in shear strength for a given lithology will emerge.

ACKNOWLEDGMENTS

The authors are thankful to all their colleagues, technical and clerical personnel who were onboard *Glomar Challenger* during Leg 31 for their help in collecting these data. Specific thanks go to Stan M. White for his encouragement to carry out this particular study.

Bruce R. Sidner critically read the manuscript and Mrs. Margie L. Dupler did all the final typing. Mark Bouma assisted in the plotting of the graphs. Their help is greatly appreciated.

Acknowledgment is made to the donors of the Petroleum Research Fund, American Chemical Society (Grant No. 2483-63) for partial support of this work at the University of California, Santa Cruz.

REFERENCES

- Bennett, R.H. and Keller, G.H., 1973. Physical properties evaluation. In van Andel, T.H., Heath, G.R., et al., Initial Reports of the Deep Sea Drilling Project, Volume 16: Washington (U.S. Government Printing Office), p. 513-519.
- Boyce, R.E., 1972a. Syringe technique and rock chunk technique. Porosity, wet-bulk density and water content: Unpublished report, June 15, Deep Sea Drilling Project.
- _____, 1972b. Cylinder technique: porosity, water content and wet-bulk density: Unpublished report, June 15, Deep Sea Drilling Project.

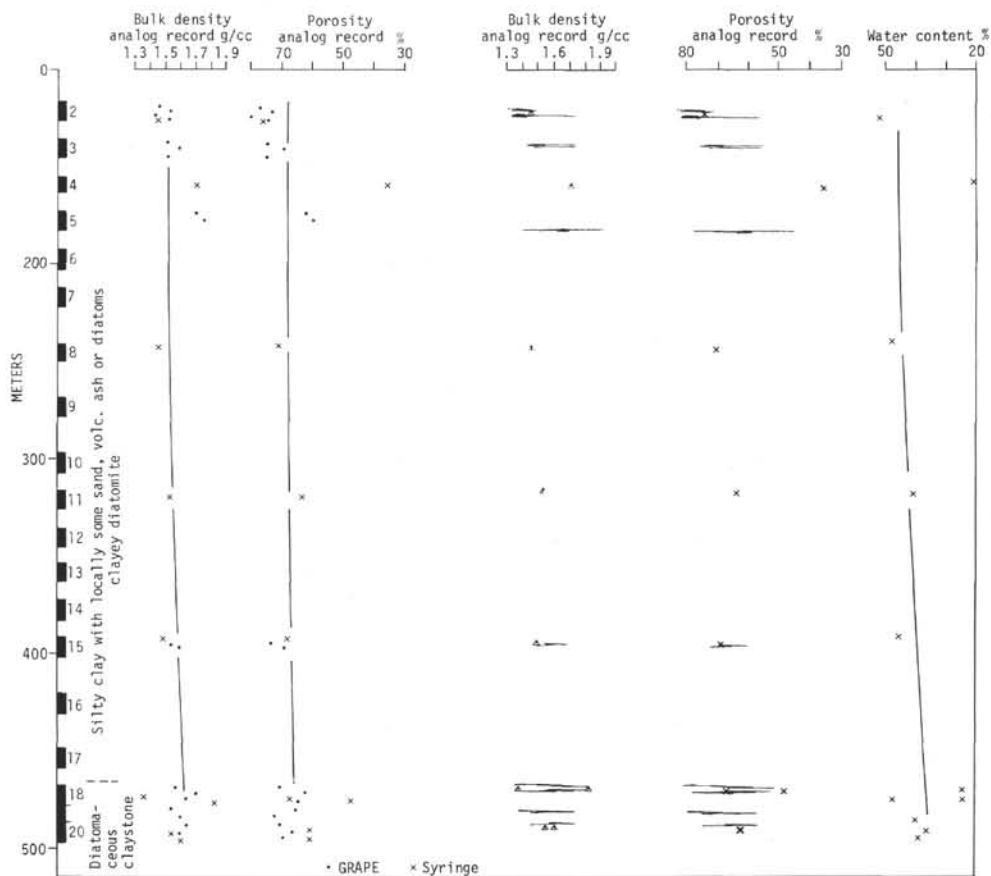


Figure 16. Plot of physical properties for Site 301. GRAPE analog record readings as well as computer plot are presented in addition to laboratory analyses (syringe and chunk methods). On the left the cores are given as black rectangles and the general lithology.

_____, 1972c. GRAPE. Memorandum to shipboard scientists responsible for physical properties aboard the *Glomar Challenger*: Unpublished report, October 12, 1972, Deep Sea Drilling Project.

_____, 1973a. Cylinder technique, attenuation coefficients, porosity, water content and wet-bulk density: Unpublished report, revised 20 April 1973, Deep Sea Drilling Project.

_____, 1973b. Discrete sampling technique, definitions and equations: Unpublished report, Deep Sea Drilling Project.

_____, 1973c. Physical properties-methods. In Edgar, N.T., Saunders, J.B., et al., Initial Reports of the Deep Sea Drilling Project, Volume 15: Washington (U.S. Government Printing Office), p. 1115-1127.

_____, 1973d. Renovated GRAPE and POROSITY-DENSITY Program: Memorandum, Deep Sea Drilling Project (to N.T. Edgar), January 11.

_____, 1973e. Wet-bulk density determination of marine sediments by gamma ray attenuation: derivation of the techniques and its use for data collected during Legs 3 through 11 of the Deep Sea Drilling Project: Unpublished Manuscript, Deep Sea Drilling Project.

_____, 1974a. Instructions for grain density, wet-bulk density, water content and porosity determinations by individual samples and gamma ray attenuation porosity evaluator: Unpublished report, January 18, 1973, revised January 16, 1974, Deep Sea Drilling Project.

_____, 1974b. Diameter problems in 2-minute count GRAPE data: Memorandum to shipboard scientists and technicians. June 3, 1974. Deep Sea Drilling Project.

Cernock, P.J., 1970. Sound velocities in Gulf of Mexico sediments as related to physical properties and simulated overburden pressures: Tech. Rept., Texas A&M Univ., Res. Found., ref. 70-5-T.

Evans, H.B., 1965. GRAPE—A device for continuous determination of material density and porosity. SPWLA Logging Symp., 6th Ann., Dallas, Texas, 1965, Trans., v. 2, p. B1-25.

Gealy, E.L., 1971. Saturated bulk density, grain density and porosity of sediment cores from the western equatorial Pacific: Leg 7, *Glomar Challenger*. In Winterer, E.L., et al., Initial Reports of the Deep Sea Drilling Project, Volume 7: Washington (U.S. Government Printing Office), p. 1081-1104.

Harms, J.C. and Choquette, P.W., 1965. Geologic evaluation of a gamma-ray porosity device. SPWLA Logging Symp., 6th Ann., Dallas, Texas, 1965, Trans., v. 2, p. C1-37.

Lee, H.J., 1973. Measurements and estimates of engineering and other physical properties, Leg 19. In Creager, J.S., Scholle, D.W., et al., Initial Reports of the Deep Sea Drilling Project, Volume 19: Washington (U.S. Government Printing Office), p. 701-719.

Manheim, F.T., Dwight, L., and Belastock, R.A., 1974. Porosity, density, grain density and related physical properties of sediments from the Red Sea drill cores. In Whitmarsh, R.B., Weser, O.E., Ross, D.A., et al., Initial Reports of the Deep Sea Drilling Project, Volume 23: Washington (U.S. Government Printing Office), p. 887-907.

TABLE 21
Bulk Density, Porosity, and Water Content as Determined by the GRAPE and Syringe Methods, Site 302

Core	Section	Diameter (in.)	Interval (cm)		Lithology	GRAPE		Syringe		Remarks				
			GRAPE ^a	Syringe		Bulk Density (g/cc)	Porosity (%)	Water Content (%)	Bulk Density (g/cc)		Porosity (%)			
2	2	2.65	A	35	Diatom-rich silty clay	1.45	79	59.18	1.33	78.66	Also volc. ash			
	5			130				Diatom-rich silty clay				48.24	1.46	70.63
				144-150				Diatom-rich silty clay				44.58	1.52	67.97
6		2.65	0-40	144-150	Diatom-rich silty clay	1.46	78							
		2.65			67-120	Diatom-rich silty clay	1.33	87						
		2.65			120-150	Diatom-rich silty clay	1.46	78						
3	2	2.65	0-60	72	Zeolite-rich clay	1.55	72							
		2.65			60-120	Rad zeolite-rich clay	1.46	78	54.19	1.40		79.06		
		2.65			120-150	Zeolite-rich clay	1.55	72						
4	3	2.65	A	75	Micarb zeolite-rich clay	1.51	75	49.38	1.50	74.20				
		2.65			0-75	55	Zeolite clay	1.56	71	48.19		1.49	71.86	
		2.65			75-100	Zeolite clay	1.50	75						
5	5	2.65	0-75	75	Zeolite clay	1.55	72							
		2.65			75-150	Zeolite clay	1.50	75						
		2.65			A	Diatom ooze	1.46	78						
5	4	2.65	A	144-150	Diatom ooze			57.71	1.36	78.29				
					Diatom ooze	1.47	77							
					Diatom ooze	1.35	85							
7	2	2.65	A	70	Diatom ooze	1.47	77							
		2.65			0-62	Diatom ooze	1.41	81	57.44	1.32	75.97			
		2.65			62-96	Diatom ooze	1.42	81	55.90	1.37	76.70			
8	5	2.65	A	75	Diatom ooze	1.34	86	62.94	1.28	80.34				
					2.65	96-150	Diatom ooze	1.36	85	60.38	1.31	79.09		
					2.65	A	75	Diatom ooze	1.36	85	60.86	1.26	76.71	
9	2	2.65	A	75	Diatom ooze	1.34	86	62.95	1.28	80.57				
					2.65	A	50	Diatom ooze	1.38	83	60.11	1.33	79.77	
					2.65	A	75	Diatom ooze	1.38	83	57.86	1.34	77.71	
10	6	2.65	A	144-150	Diatom ooze	1.37	84	61.91	1.30	80.74				
					2.65	A	75	Diatom ooze	1.37	84	61.27	1.28	78.51	
					2.65	A	75	Diatom ooze	1.41	81	57.49	1.31	75.13	
11	4	2.65	A	144-150	Diatom ooze	1.42	81	55.48	1.36	75.43				
					2.65	A	75	Diatom ooze	1.37	84	58.37	1.31	76.43	
					2.65	A	75	Diatom ooze	1.37	84	57.95	1.34	77.68	
12	2	2.65	A	75	Diatom ooze	1.37	84	57.12	1.32	76.46				
					2.65	A	75	Diatom ooze	1.37	84	57.95	1.34	77.68	
					2.65	A	75	Diatom ooze	1.37	84	57.12	1.32	76.46	
13	4	2.65	A	144-150	Diatom ooze			38.38	1.57	60.11				
					2.65	A	75	Zeolite-rich clay	1.37	84				
					2.65	A	75	Zeolite-rich clay	1.35	85				
14	2	2.65	A	75	Zeolite-rich clay									
					2.35	piece								
					2.37	piece								
17	1	2.35	piece	144-150	Zeolite-rich clay									
					2.37	piece								
					2.37	piece								
17	2	2.35	piece	144-150	Zeolite-rich clay									
					2.37	piece								
					2.37	piece								
17	2	2.35	piece	144-150	Zeolite-rich clay									
					2.37	piece								
					2.37	piece								

^aA = average reading from the GRAPE analog record.

Roth, P.H. and Thierstein, H., 1972. Calcareous nannoplankton. In Hayes, D.E., Pimm, A.C., et al., Initial Reports of the Deep Sea Drilling Project, Volume 14: Washington (U.S. Government Printing Office), p. 421-481.

Schlumberger, 1966. The formation Density Log. In Schlumberger log interpretation principles. Paris (Kecran-Servant (23827)), p. 47-49.

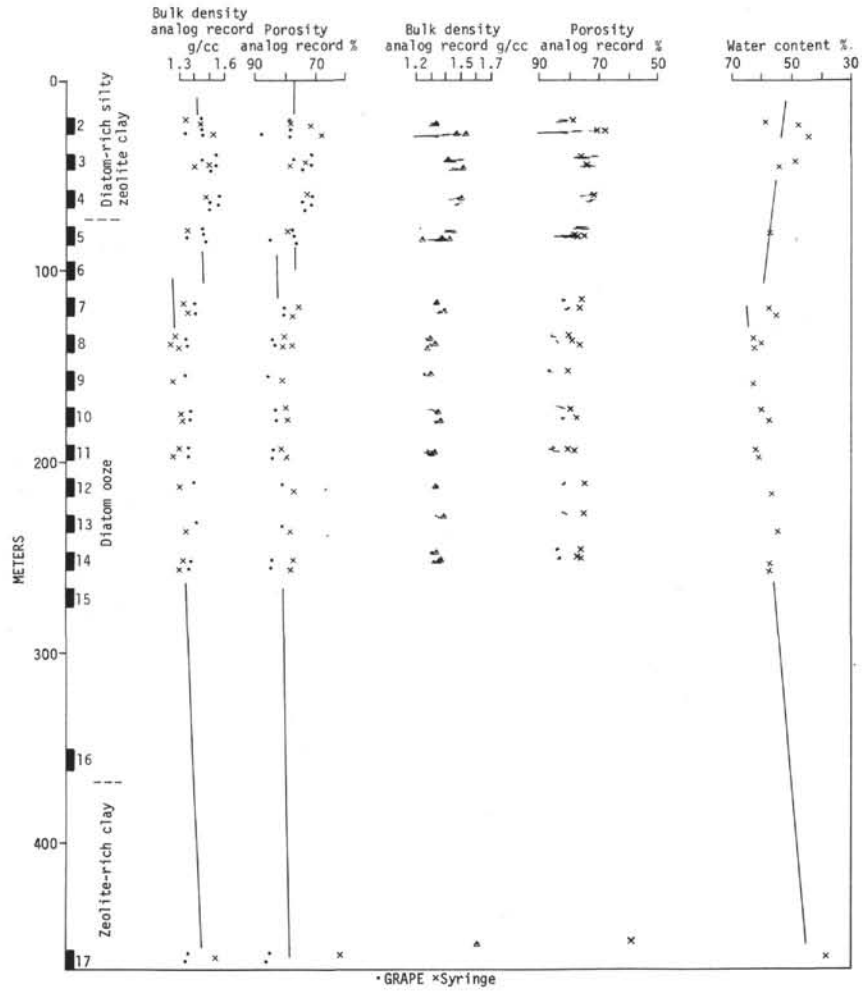


Figure 17. Plot of physical properties for Site 302. GRAPE analog record readings as well as computer plot are presented in addition to laboratory analyses (syringe and chunk methods). On the left the cores are given as black rectangles and the general lithology.

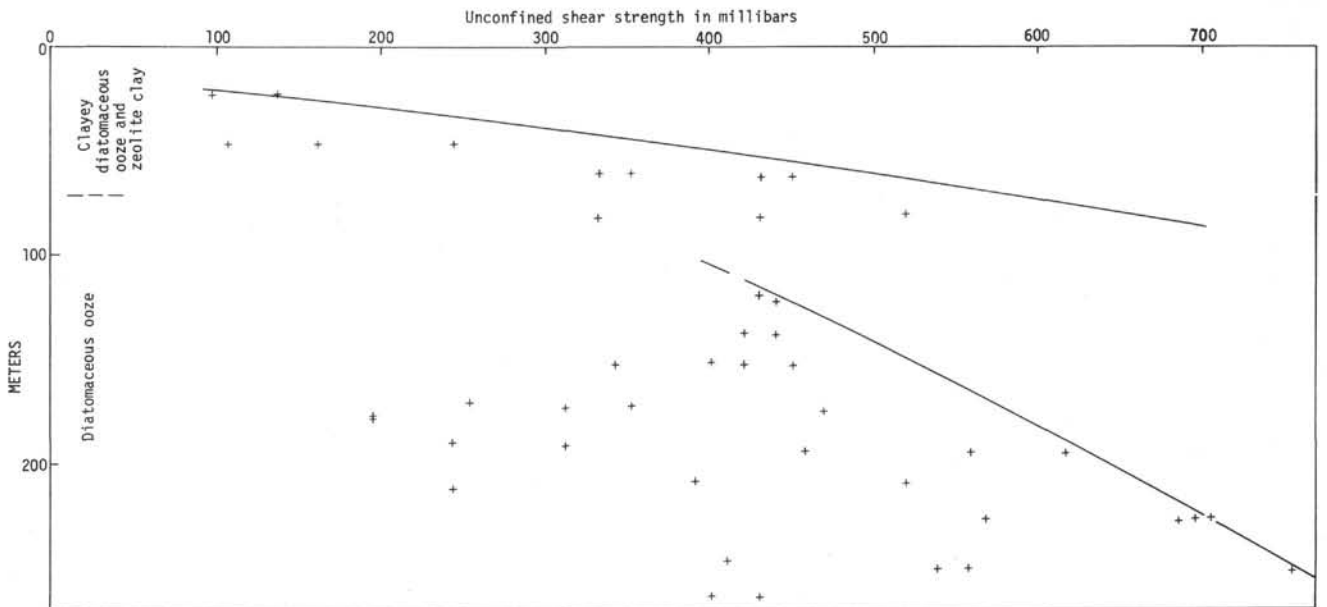


Figure 18. Plot of unconfined shear strength with depth, Site 302.

TABLE 22
Vane Shear Data, Site 302

Sample (Interval in cm)	Depth (to nearest half meter)	Plane of Measurement	Shear Strength (mbar)
2-4, 10	24.0	Vertical	97.6
2-3, 140	24.0	Vertical	136.6
3-6, 100	47.0	Vertical	162.0
3-6, 50	46.5	Vertical	244.0
3-6, 145	47.5	Vertical	107.4
4-3, 100	63.0	Vertical	351.4
4-3, 135	63.5	Vertical	331.8
4-4, 140	65.0	Vertical	429.4
4-4, 135	65.0	Vertical	448.9
5-3, 145	82.5	Vertical	517.3
5-4, 145	84.0	Vertical	429.4
5-5, 100	85.0	Vertical	331.8
5-5, 120	85.0	Vertical	683.2
7-4, 140	120.5	Vertical	429.4
7-6, 140	123.5	Vertical	439.2
8-4, 26	138.0	Vertical	419.7
8-4, 106	139.0	Vertical	439.2
9-1, 86	159.5	Vertical	400.2
9-1, 135	160.0	Vertical	419.7
9-2, 22	160.0	Vertical	341.6
9-2, 111	161.0	Vertical	448.9
10-1, 87	172.5	Vertical	253.8
10-2, 87	174.0	Vertical	351.8
10-3, 56	175.0	Vertical	312.3
10-4, 87	177.0	Vertical	468.0
10-5, 92	178.5	Vertical	195.2
10-6, 76	180.0	Vertical	195.2
11-2, 72	194.0	Vertical	244.0
11-3, 74	195.5	Vertical	312.3
11-5, 20	198.0	Vertical	456.7
11-5, 75	199.0	Vertical	556.3
11-5, 121	199.0	Vertical	614.8
12-2, 42	214.5	Vertical	390.4
12-3, 42	216.0	Vertical	517.3
12-4, 37	217.5	Vertical	244.0
12-4, 115	218.0	Vertical	244.0
13-1, 83	235.5	Vertical	702.7
13-1, 136	236.0	Vertical	566.1
13-2, 30	236.5	Vertical	693.0
13-2, 108	237.0	Vertical	683.2
14-2, 89	251.5	Vertical	409.9
14-5, 17	255.0	Vertical	556.3
14-5, 65	255.5	Vertical	536.8
14-5, 127	256.5	Vertical	751.5
15-1, 70	274.5	Vertical	400.2
15-1, 124	275.0	Vertical	429.4
16-1, 140	361.0	Vertical	927.2

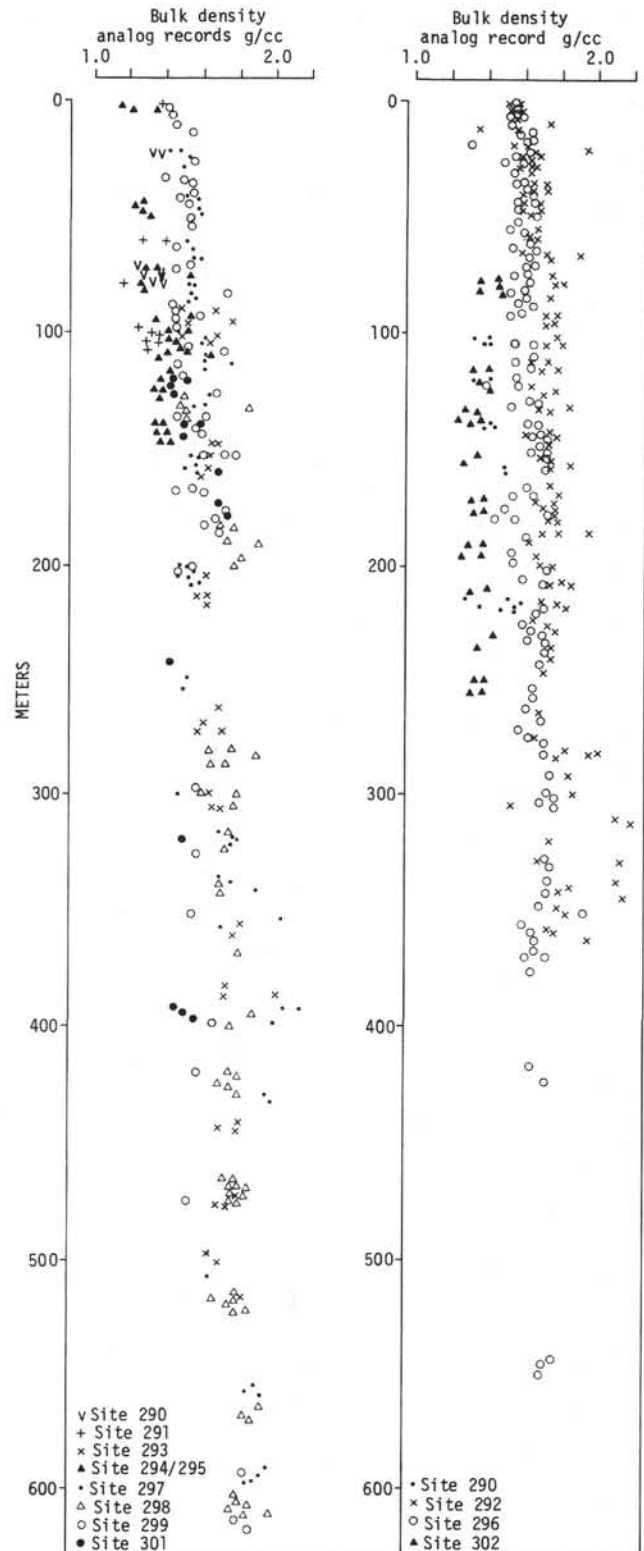


Figure 19. Plots of bulk densities obtained from GRAPE analog records for all sites of Leg 31, grouped according to major lithologies. For explanation, see text.

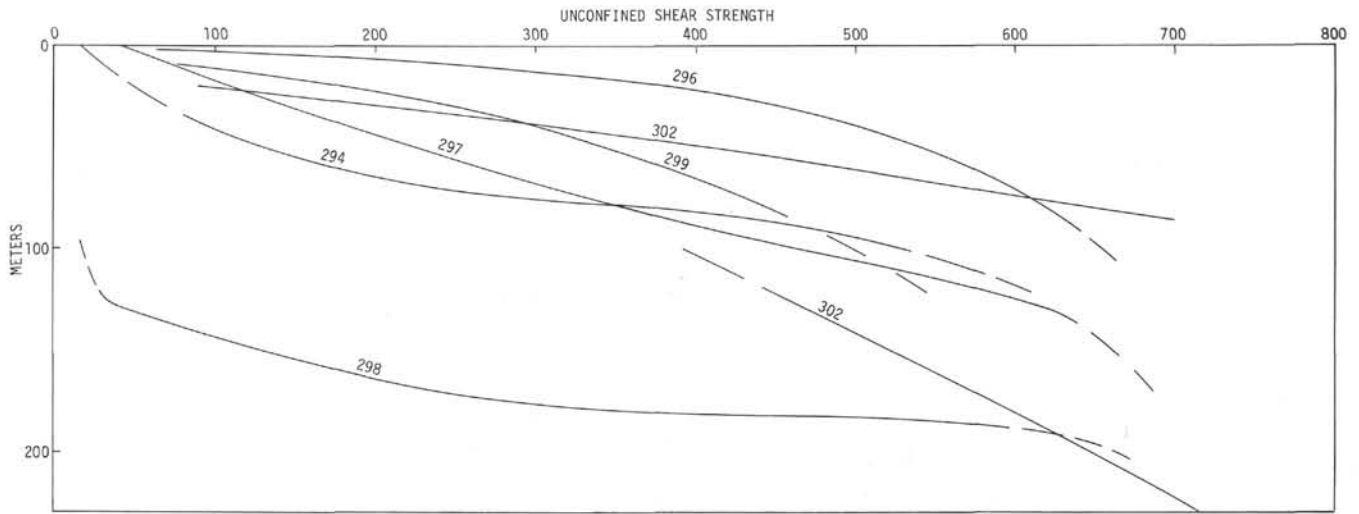


Figure 20. Summary of enveloping curves for all shear strength data for Leg 31.

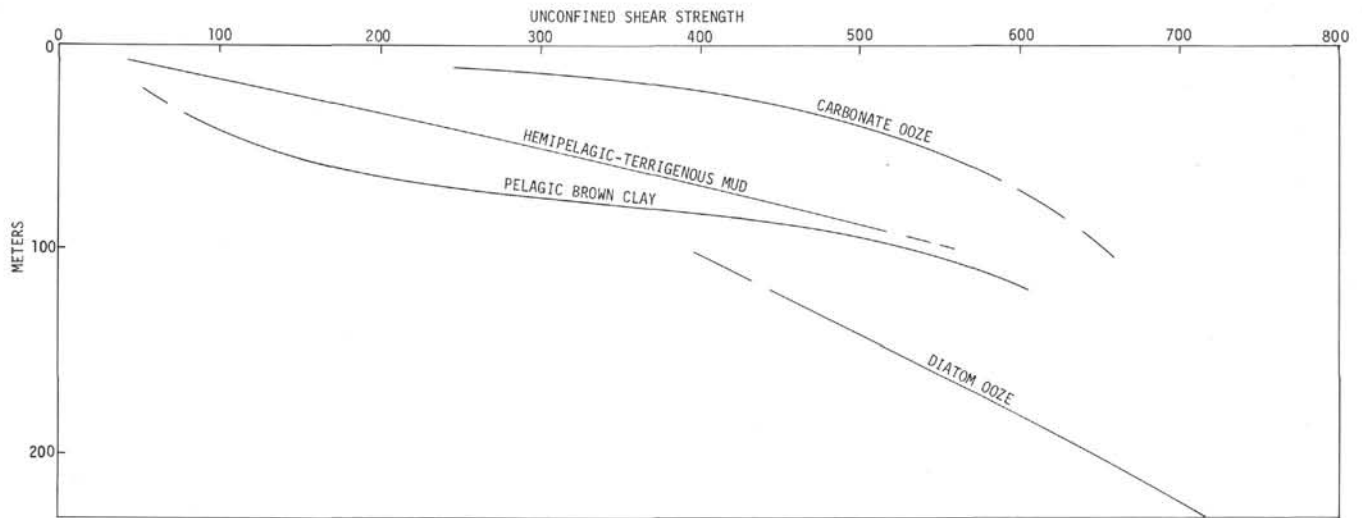


Figure 21. Summary of enveloping curves for shear strength characterized by homogeneous lithology. Carbonate ooze (Site 296), hemipelagic-terrigenous mud (average Sites 297, 299, 302—upper portion), pelagic brown mud (Site 294), diatom ooze (Site 302—lower portion).

TABLE 23
Shear Strength of Diatom Ooze, Pelagic Brown Clay, Hemipelagic-Terrigenous Mud, and Carbonate Ooze

Depth (m)	Diatom Ooze	Pelagic Brown Clay	Hemipelagic-terrigenous Mud	Carbonate Ooze
50	—	125	300	538
	—	0	140	330
100	390	535	560	650
	0	37	44	67

Note: Absolute strength indicated in mbar. Shear strength of lithology increases from left to right. Relative increase in strength (as % over weakest lithology at given depth) also indicated.